IEEE Access
Multidisciplinary ⋮ Rapid Review ⋮ Open Access Journal

Received 17 January 2024, accepted 28 January 2024, date of publication 1 February 2024, date of current version 7 February 2024.

Digital Object Identifier 10.1109/ACCESS.2024.3361038

RESEARCH ARTICLE

Investigations on Secrecy Performance of Downlink Overlay CR-NOMA System With SIC Imperfections

KIRAN KUMAR GODUGU, (Graduate Student Member, IEEE), AND SUSEELA VAPPANGI, (Member, IEEE)
School of Electronics Engineering, VIT-AP University, Amaravati, Andhra Pradesh 522237, India
Corresponding author: Suseela Vappangi (suseela.v@vitap.ac.in)

ABSTRACT Cognitive radio (CR) and non-orthogonal multiple access (NOMA) are two technologies witnessed to offer tremendous possibilities for the next generation wireless networks to maximise their usage of available spectrum. In this work, we evaluate the performance of a downlink overlay secure CR-NOMA system while the secondary transmitter (ST) is used as a decode-and-forward (DF) relay to assist the primary transmitter (PT) to transmit information to the destination i.e., primary user (PU), while covertly transmitting its own information to the secondary user (SU) against the eavesdropper (Eve) of PT. The secrecy performance comparison between two users i.e., PU and SU are obtained under perfect and imperfect successive interference cancellation (SIC), respectively. Furthermore, this paper investigates the secrecy performance comparison between the proposed overlay downlink CR-NOMA system comprising of single antenna (SA) and multiple antennas (MA) in terms of various performance metrics such as secrecy sum rate (SSR), the average secrecy rate (ASR), the average secrecy sum rate (ASSR), strictly positive secrecy rate (SPSC) and secrecy outage probability (SOP). It is to be noted that in our proposed system, MAs are equipped at both PT and ST with the main purpose to provide cooperative diversity and we employ both maximal ratio combining (MRC) and selection combining (SC) diversity techniques for processing the received signals at the PU/Eve which further improves the system's capacity and enhances the secrecy performance. In addition, for characterizing the secrecy performance of the proposed overlay CR-NOMA network, we present thoroughly the derivations of novel closed-form analytical expressions of the performance metrics such as SOP, SPSC and the ASR by taking into account both perfect SIC (pSIC) and imperfect SIC (ipSIC) scenarios. Based on the analytical frameworks, the numerical and simulation results are obtained under different network parameters. Towards this end, the outcomes of the simulation are shown to prove both the reliability of the mathematical analysis and the accuracy of the suggested technique.

INDEX TERMS Non-orthogonal multiple access, physical layer security, overlay cognitive radio, secrecy rate, average secrecy rate, strictly positive secrecy rate.

I. INTRODUCTION

The rapid emergence of a diverse variety of applications such as the internet of things (IoT), virtual reality (VR), augmented reality (AI), unmanned aerial vehicles (UAV), autonomous driving, live video streaming, online gaming, video conferences, etc., is posing an unprecedented ultimatum for the fifth generation (5G) and future generations of wireless networks to cater the needs of the end users. More particularly, the 5G and beyond 5G (B5G) wireless networks suffer from spectrum limitations due to this explosive increase in mobile traffic and high-rate data transmission capabilities. In a limited bandwidth, it is of utmost necessity for the network providers to take into consideration several aspects such as massive connectedness, ultra-low latency, extremely high throughput, improved user fairness, etc.

The associate editor coordinating the review of this manuscript and approving it for publication was Barbara Masini.

Thus, in this context, with the major motive to address the aforementioned demands, rapid advancements in the utilization of multiple access techniques among all the generations of cellular communication systems starting from first generation i.e., (1G) through 4G such as the frequency division multiple access (FDMA), time division multiple access (TDMA), code division multiple access (CDMA), and orthogonal frequency division multiple access (OFDMA) can be witnessed. However, these multiple access techniques rely on the same concept called orthogonality which implies that users share the resources in an orthogonal manner i.e., each of the users is allowed to utilize exclusively an orthogonal resource block i.e., either a frequency channel, time slot, spreading code, etc. The major drawback associated with the utilization of these schemes is that they lead to significant limitations on the total number of users that can access the spectrum thus curtailing the spectral efficiency.

Eventually, non-orthogonal multiple access (NOMA) has gained a substantial amount of recognition to facilitate effective utilization of spectral resources. Particularly, NOMA circumvents the drawback of the aforementioned OMA techniques by serving an arbitrary number of users contemporaneously within the same frequency band. Generally, NOMA employs the phenomena of power domain multiplexing for superimposing multiple user signals within the same time-frequency resource blocks. A list of earlier studies affirms that NOMA exhibits the potential to be easily integrated with other existing communication technologies. Hence, it has been included in 3rd generation partnership project (3GPP) where NOMA is ably known as multi-user superposition transmission (MUST). Apart from this, NOMA has been incorporated in the digital TV standard ATSC 3.0 where it is specified as layered division multiplexing (LDM). Notably, upon using the principle mechanism of NOMA, where multiple data streams are superimposed, the spectral efficiency of TV broadcasting can be enhanced. Thus, these examples clearly manifest the enormous caliber of NOMA which confirms its incorporation in future wireless communication systems.

Besides, cognitive radio (CR) also offers a platform for effective utilization of the wireless spectrum where the secondary users (SUs) also known as CR users are allowed to opportunistically access the band of spectrum occupied by the primary users (PUs) by adopting three different paradigms such as the interweave, underlay and overlay. The spectrum sharing strategy which we focus in this paper is overlay. In all of these three mechanisms, SUs are allowed to occupy the spectrum of PUs only upon ensuring that they do not hinder the quality of service (QoS) of the primary user. Apparently, in order to facilitate the sharing of the spectrum in an intriguing manner, one simple solution is to integrate the prospects of NOMA with CR. More specifically the prevailing research articles demonstrate that the amalgamation of NOMA with CR satisfies several necessities of the future wireless networks such as the assurance of low latency, massive connectivity, high data transfer, etc. In this work we integrate the concepts of NOMA to the overlay CR system. Recently published studies have shown that CR-NOMA systems can meet 5G/B5G network requirements such as huge connection, low latency, and high throughput [1], [2], [3], [4], [5]. In the overlay spectrum sharing mechanism, the secondary transmitter is allowed to cooperate with the primary transmitter and aids in relaying the information of the primary user in contemplation of sharing the licensed primary user's spectrum and it is given a privilege to transmit its own signal as well. While developing any wireless communication systems, it is of utmost necessary to assure adequate amount of security. However, the broadcast nature of the wireless communication channel is resulting the wireless system to become susceptible to the adverse effects of eavesdropping. This threat is more pronounced in a CR system due to the fact that there is a lot more chance for such systems to get wiretapped when facilitating the unlicensed users especially the malignant users to access the spectrum occupied by the primary or licensed users. To circumvent such threats, several cryptographic algorithms and secret keys have been proposed to enhance the security of the transmitted information. Nonetheless, these encryption and decryption algorithms involve a lot of computational complexity. Thus, physical layer security (PLS) has emerged out as an excellent counterpart to guarantee with substantial amount of security at the physical layer. In addition, PLS which has been the subject of intense research to improve wireless system security, and it can also be used to secure NOMA [6], [7]. In this work, we address the PLS aspects of overlay CR-NOMA system by taking into consideration both perfect and imperfect successive interference cancellation (SIC) scenarios. In [8], the PLS aspects of an underlay CRN is evaluated with respect to secrecy outage probability (SOP), average secrecy rate (ASR), and quantity of secrecy loss (ASL). From this work, it can be affirmed that the authors derived closed-form expressions of SOP, ASR, and ASL over imperfect channel state information (CSI) with Rayleigh fading, where the wiretap channels and the legitimate channels are correlated.

A. RELATED WORKS

Two uplink NOMA systems, one is the random jammer selection based uplink NOMA transmission (RJS-UNT) method that does not require knowledge of the eavesdropper's CSI, and the other one is optimal jammer selection based uplink NOMA transmission (OJS-UNT) method that makes use of the eavesdropper's CSI when it is available, are proposed in the work discussed in [9]. In addition, we compare this approach with another scheme called a non-jammer selection based uplink NOMA transmission (NJS-UNT) method that doesn't rely on jammer selection to function. In order to measure how well these systems keep secrets, we create analytical formulations for the SOP. The results demonstrate that the schemes get closer to SOP levels as the signal-to-noise ratio (SNR) improves. When compared to the

NJS-UNT scheme, the SOP floors achieved by the RJS-UNT and OJS-UNT are substantially lower. This is indicative of the system's superiority in terms of security. While the authors in [10] are mainly concerned to enhance the security of confidential information transmission between a source, two destinations, a friendly jammer (FJ), and an eavesdropper (Eve). To thwart Eve's attempts to intercept data, the FJ sends a jamming signal concurrently with the source sending a superimposed signal across both receivers that through NOMA. Both users are aware of the jamming signal and subtract it from the received signal before decoding the information using the NOMA technique. Further, the authors in this work focus on the analysis of SOP, which varies based on the different target secrecy rates of the two users.

The research work in [11] explores the application of NOMA in large-scale underlay CR networks with randomly deployed users. Predominantly, underlay CR networks operate on the principle that SUs can utilize the PU's spectrum, provided they adhere to a predefined interference threshold within the primary network (PN). This concept allows SUs to access PU spectrum resources without causing significant disruption to the primary users. The authors in [11] focuses on characterizing network performance by deriving new closed-form expressions for outage probability (OP) through stochastic geometry. The study distinguishes between two power constraint cases: 1) fixed transmit power for primary transmitters (PTs) and 2) PT's transmit power proportional to that of the secondary base station (SBS). In case-1, NOMA users experience a diversity order of 'm' at the m^{th}-ordered user, suggesting improved performance. However, in case-2, an asymptotic error level is observed for the OP, indicating limitations. The authors of the article quoted in [12] investigated a cooperative underlay CR-NOMA framework with a single relay. This system enables multiple SUs to send and receive signals concurrently while still adhering to primary interference power limitations. The work in [13] explores the performance of a NOMA based underlay CR framework with partial relay selection (PRS). In this setup, the secondary network employs NOMA, utilizing K half-duplex (HD), decode-and-forward (DF) relays to assist the SBS in serving SUs. This study presents closed-form solutions for OPs obtained by SUs under erroneous SIC conditions, while also considering interference thresholds for primary receivers and maximum transmit power constraints for secondary nodes.

An overlay CR-NOMA framework with a single relay was taken into consideration by the authors in [14]. This research article examines an overlay CR-NOMA framework that operates under the secrecy constraint imposed by PUs. In this network, secondary transmitters assist in relaying primary users' messages in exchange for access to the primary user's spectrum. The major focus of the work as stated in [14] is to assess the secrecy performance of primary users while treating secondary users as potential eavesdroppers. It highlights the need to adjust the power allocation between primary and secondary users to enhance security. Notably, the proposed scheme involves the consideration of multiple primary users who are paired based on their channel gains. This pairing enables the implementation of NOMA protocols to enhance the overall system performance. The work in [15] focuses on the relay selection issue in cognitive radio networks that operate within a spectrum-sharing framework. The SUs in the CR-NOMA framework opportunistically tap into licensed spectral gaps to increase the number of accessible SUs, which is vital given the limited and dynamic nature of available spectrum. To enhance the effectiveness of distant users, a PRS architecture is employed for both full-duplex (FD) and HD relays in both uplink and downlink communications. Furthermore, this work provides analytical expressions for OPs in FD and HD relay-aided CR-NOMA frameworks. Additionally, analytical expressions for asymptotic OPs and ergodic capacity (EC) are derived, shedding light on key factors influencing CR-NOMA network performance. Extensive simulations validate the effectiveness of these closed-form solutions, demonstrating their applicability to FD and HD relay-aided CR-NOMA frameworks.

B. MOTIVATIONS AND CONTRIBUTIONS

In [16], the authors examined a multi-user cooperating overlay CR-NOMA system with imperfect SIC and imperfect CSI. By taking into consideration both imperfect SIC/CSI scenarios, the authors computed the end-to-end OP and capacities of both the primary and secondary networks. In [17], the closed-form equations for the end-to-end OP of the cooperative underlay CR-NOMA DF relaying networks across Rayleigh fading with the PU interference and incomplete CSI were developed. However, the work in [18] is similar to that of [17] where they were investigated OP of cooperative CR-NOMA system with imperfect SIC. In [19], the OPs and ECs for every pair of signals under the assumption of erroneous SIC and co-channel interference (CCI) were obtained as closed-form solutions in conjunction with the basic functions. Above all research works have not discussed any security methods and this motives us to incorporate PLS to improve system's secrecy performance under the presence of external or passive eavesdropper node in our proposed work. In [4], the authors have examined the OP and throughput of overlay cognitive NOMA system with imperfect SIC (ipSIC). In their work, the authors have performed asymptotic analysis and attained the closed-form OP expressions of PU and SU when their transmit SNRs approaches infinity. Furthermore, the simulation results of this work demonstrated that overlay CR-NOMA system outperforms overlay CR-orthogonal multiple access (OMA) and underlay CR systems via SU's OP performance and system throughput. However, the authors have not considered PLS aspects and this motivates us to do the necessity.

In [21], the researchers explored PLS based cooperative downlink NOMA system employing a HD relay in the context of an external eavesdropper (Eve). To ensure secured communication, a two-stage jammer approach was offered. In addition, they have evaluated the secrecy of the system in

terms of the closed-form solutions of SOP for two trusted users. To improve transmission and achieve diversity gain, multi-antenna relays have been extensively deployed. The ability of Rician fading channels to conceal information is studied in [24]. In specifically, the probability of having a strictly positive secrecy capacity (SPSC) is obtained in a closed-form expression. In [25], the authors have studied how well an uplink NOMA preserved information private for both single antenna (SA) and multiple antenna (MA) users. Also, the authors have analyzed the PLS performance in terms of SOP and SPSC. However, all these aforementioned research works are confined to analyzing the performance of cooperative NOMA system under imperfect SIC assumptions but they have not considered CR-NOMA systems.

In order to study the effect of SIC on real-world detectors, the authors in [30] present a new generalized residual interference (RI) approach. They used the proposed method to analyze RI at receivers in a two-user untrusted NOMA network and found the analytical and asymptotic formulations of SOP for both users. According to the authors in [31], the SOP performance of CR-NOMA system is investigated using a hybrid SIC and power control (HSIC-PC) approach. The exact and asymptotic SOP of SU were found using mathematical calculations. To further improve the SU's SOP, the HSIC-PC-artificial-noise (HSIC-PC-AN) method was also suggested. According to the research work as shown in [32] investigates the PLS of an OCRN with a strong PT operating under a peak interference power limitation. The capacity for outages, intercept probability, and SOP in passive eavesdropping are all expressed mathematically. New expressions for the exact and approximate average secrecy capacity (ASC) for active eavesdropping have been found after extensive research on the ASC. In order to enhance SR and examine IRS-aided NOMA PLS, the researchers of [33] suggested a realistic situation with IRS-assisted NOMA which involves barriers that hinder direct transmission among the base station (BS), users, and an eavesdropper. They derive a closed form expression for the ergodic secrecy rate, and the numerical data indicate that the system's performance can be enhanced by incorporating IRS elements.

The subject of secret communications among RIS-NOMA frameworks was investigated in [34] using on-off controls. For the k^{th} legitimate user (LU) in RIS-NOMA networks, novel approximative and asymptotic SOP formulations were generated utilizing ipSIC/pSIC. As compared to RIS-OMA, AF relaying, and HD/FD DF relaying, these equations are far better. On top of it, the authors have come up with solutions for the secrecy system throughput in delay-limited transmission mode. The PLS has been mentioned about in context of a big NOMA framework that uses both FD and AN techniques in [35]. It was also possible to make a safe joint communication approach. In this system, NOMA users that are nearby and working in FD state mess up other signals and boost the PLS of the LU signal by making fake noise. For a certain set of users, one learns a closed-form answer based on the SOP. In [36], the authors explained how to set up a new DF-aided joint NOMA structure with two people which functions in both HD and FD states. Different types of SOP closed-form expressions have been made using the HD and FD methods. Two different ways of sending information have been suggested in [37] as ways to make the two-way relay (TWR) method with the listener more private. The analytical expressions of OP and intercept probability (IP) have been found. A numerical simulation was used to make sure that the mathematical findings were correct. The PLS of the simultaneously sending and reflecting (STAR)-RIS-NOMA was analyzed in [38]. The randomized geometry-based technique was employed for modeling random locations of the Eves and NOMA legitimate users (LUs). The authors in [38] have derived the mathematical forms of the SOP and the ASC for the time-splitting (TS) and energy-splitting (ES) protocols when the SIC order of the NOMA LUs is based on the channel gains.

In a millimeter wave (mmWave) beamspace MIMO system, the employment of UAVs equipped with lens antenna arrays (LAAs) is contemplated in [39] as a means to facilitate multi-user transmission. In order to minimize the number of RF chains, a UAV-enabled multiuser MIMO system that combines the UAV's altitude design with hybrid beamspace precoding is suggested. A minimum weighted mean squared error (MWMSE) approach is used to construct the optimization issue in the suggested approach. To achieve efficient and flexible coverage in mmWave UAV telecommunications, the contributors of [40] suggested a three-dimensional (3D) beamforming method. They achieve a smallest rectangular that will encompass the target area by taking the coordinate transformation of the target region. Then, they have achieved an extensible coverage. Afterwards, a broad beam is designed to span the rectangular using the sub-array approach.

Inspired by the previously mentioned concerns, we introduce a PLS based overlay CR-NOMA downlink system which is equipped with SA as well as MA at the primary/secondary transmitters to perform a reliable transmission for two users under perfect and imperfect SIC assumptions. The following is a brief overview of our main contributions:

1) The proposed PLS based overlay CR inspired downlink NOMA (CR-NOMA) system with two primary/secondary transceivers, and one eavesdropper is configured along with artificial noise aided jamming signals to improve the security of the system, where, the eavesdropper is having the ability to detect both NOMA users simultaneously.
2) For the proposed overlay CR-NOMA system, the system diversity has been improved by incorporating both maximal ratio combining (MRC)/selection combining (SC) techniques for processing the received signal, and this work also derives the novel closed-form solutions for the average secrecy rate (ASR), strictly positive secrecy rate (SPSC) and SOP under both perfect SIC (pSIC) and ipSIC scenarios.

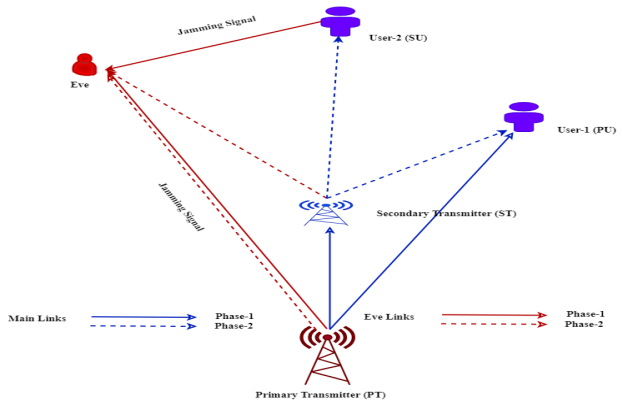

FIGURE 1. Proposed network model: Overlay secure CR-NOMA network.

3) By taking into consideration different network parameters such as transmit SNR, user target rates, and residual interference due to ipSIC, this work provides a secrecy performance comparison between both primary/secondary users (PU/SU).
4) Further, the secrecy performance of the proposed overlay secure CR-NOMA network is improved by exploiting the multiple antennas (MA) at the primary/secondary transmitters and also analyzes the performance of PU for both exact/asymptotic behaviors for different network parameters.

C. ORGANIZATION OF PAPER

Followed up by the introduction section, the rest part of this paper is organized as follows: Section II introduces the PLS aspects in the two user overlay downlink CR-NOMA system which is making use of SA. In Section III, we present a detailed analytical derivations of SOP/SPSC, ASR, and ASSR, respectively. Section IV elaborates the overlay CR-NOMA system in which the Pt/ST transmitters are making use of multiple antennas along with its extended secrecy performance analysis. Section V illustrates the simulation outcomes and observations. In Section V, we wrap up our study and draw conclusions.

II. PROPOSED NETWORK MODEL WITH SINGLE TRANSMIT ANTENNAS

The suggested network model for an overlay downlink CR-NOMA network which is equipped with single trasnmit/receive antennas at all the nodes is illustrated in Fig 1,. The above framework utilizes the NOMA techniques for the downlink communication and has a primary transmitter (PT), a primary user (PU), a secondary transmitter (ST), a secondary user (SU), and an outside listener (Eve). Since the PU is nearest to the PT and the SU is more distant, everyone of the nodes have a single transmitter which operates in half-duplex (HD) manner. Obviously, we expect that each channel will be exhibiting Rayleigh distributions. Additionally, we presume all of the channels will have additive white Gaussian noise (AWGN) having a mean of zero and a variance of σ^2. Where, h_{ij} represents the channel's fading parameter. For each i that is in the set $\{s, p\}$, The complex Gaussian random variable $j \in \{s, p, E\}$ has a mean of zero and a variance of λ_{ij}. The channel gain $|h_{ij}|^2$ follows an exponential distribution with parameter $\frac{1}{\lambda_{ij}}$.

Although thinking about privacy, remain in the fact that an eavesdropper can listen in on U_1, U_2, and ST's interactions. When receiving signals, there exist two primary phases. In this HD communication, we shall pretend that every node utilizes one antenna for trasnmission as well as reception. The x_p and x_s indicates the information signals of the PU and SU, accordingly. The sum of the values at PT and ST is the transmit power, denoted as P. The role of ST as a DF relay ensures that x_p can reach PU in an overlay secure CR-NOMA system. Because of the NOMA technique, ST is able to transmit its own signal x_s simultaneously, which is a major advantage. There are two equal stages that occur during communication as follows:

A. TRANSMISSION PHASE-I

In the first transmission phase i.e., Ph-I, x_p is transmitted by PT and at the same time SU sends jamming signal to confound Eve, since the distance between PU and Eve is greater than the distance between SU and Eve. The received signal at PU, ST, and Eve is given as [4], [5], [6], [7], [8], [9], [10], [11], [12], [13], [14], [15], [16], [17], [18], [19], [20], [21]:

$$y_{PU}^{(1)} = h_{pp}\sqrt{P}x_p + n_{PU}^{(1)} \tag{1}$$
$$y_{ST}^{(1)} = h_{ps}\sqrt{P}x_p + n_{ST}^{(1)} \tag{2}$$
$$y_{E}^{(1)} = h_{pe}\sqrt{P}x_p + h_{sue}\sqrt{P_j}w + n_{E}^{(1)} \tag{3}$$

where h_{pp}, h_{ps}, h_{pe}, and h_{sue} are the channel gains between the PT to PU, PT to ST, PT to Eve, and SU to Eve, respectively. $n_{PU}^{(1)}$, $n_{ST}^{(1)}$, $n_{E}^{(1)}$ are the noises during TS-1 at PU, ST, Eve, respectively. The signal-to-interference-plus-noise ratio (SINR) at the ST/PU to receive signal from PT, respectively, given as [4], [5], [6], [7], [8], [9], [10], [11], [12], [13], [14], [15], [16], [17], [18], [19], [20], [21]:

$$\gamma_{PU}^{(1)x_p} = \rho|h_{pp}|^2 \tag{4}$$
$$\gamma_{ST}^{(1)x_p} = \rho|h_{ps}|^2 \tag{5}$$

where ρ $(= \frac{P}{\sigma^2})$ is the transmit SNR. We assume the wiretap is capable of tracking multiple users simultaneously (MUD). In specifically, the Eve uses a parallel interference cancellation (PIC) approach to decipher the combined U_i signal. Therefore, the Eve's SINR for decoding U_i's signal can be expressed as [4], [5], [6], [7], [8], [9], [10], [11], [12], [13], [14], [15], [16], [17], [18], [19], [20], [21]:

$$*20c\gamma_{E}^{(1)x_p} = \frac{\rho_E|h_{pe}|^2}{1+\rho_j|h_{sue}|^2} \tag{6}$$

where ρ_E $(= \frac{P}{\sigma_E^2})$ is SNR at the Eve and ρ_j $(= P_j/\sigma^2)$ is the transmit SNR of jamming signal.

TABLE 1. The various symbols and their notations.

Notation	Its Description
P	Transmit Power
P_j	Jamming Signal Power
σ^2	Noise Variance
σ_E^2	Noise Variance at Eve
ρ	Transmit SNR
ρ_j	Transmit SNR of the Jamming Signal
ρ_E	SNR at the Eve
σ^2	Noise Variance
σ_E^2	Noise Variance at Eve
w	Jamming Signal
$\lvert h_{ps,M}\rvert^2$	Channel gain between PT and ST with M transmit antennas
$\lvert h_{ss,N}\rvert^2$	Channel gain between ST and SU with N transmit antennas
$\lvert h_{pp,M}\rvert^2$	Channel gain between PT and PU with M transmit antennas
$\lvert h_{sp,N}\rvert^2$	Channel gain between ST and PU with N transmit antennas

B. TRANSMISSION PHASE-II

During second transmission phase i.e., Ph-II, ST after successfully decoding x_p, it combines x_p with its own message x_s using the NOMA approach. Then ST forwards the superimposed mixer i.e., $\sqrt{a_1 P}x_p + \sqrt{a_2 P}x_s$ to PU, and SU simultaneously. In NOMA theory, as the weak users (here SU) are given a greater share of the available power, i.e., $a_2 > a_1$ (a_1 & a_1 are the power allocation (PA) factors) with $a_2 + a_1 = 1$. The received signal at PU/SU during phase-II is given as,

$$y_{PU}^{(2)} = h_{sp}\left(\sqrt{a_1 P}x_p + \sqrt{a_2 P}x_s\right) + n_{PU}^{(2)} \tag{7}$$

$$y_{SU}^{(2)} = h_{ss}\left(\sqrt{a_1 P}x_p + \sqrt{a_2 P}x_s\right) + n_{SU}^{(2)} \tag{8}$$

For the eavesdropper, during TS-2 the BS transmits a jamming signal with power P_j. It eavesdrops on the superimposed signal of PU and SU, and these can be characterised as,

$$y_E^{(2)} = h_{se}\left(\sqrt{a_1 P}x_p + \sqrt{a_2 P}x_s\right) + h_{pe}\sqrt{P_j}w + n_E^{(2)} \tag{9}$$

where $n_{PU}^{(2)}$, $n_{SU}^{(2)}$, $n_E^{(2)}$ are the noises during TS-2 at SU, PU, Eve respectively. The SINR at the SU/PU/Eve to receive signal from ST, respectively, given as [4], [5], [6], [7], [8], [9], [10], [11], [12], [13], [14], [15], [16], [17], [18], [19], [20], [21]:

$$\gamma_{SU}^{(2)x_s} = \frac{a_2\rho|h_{ss}|^2}{1 + a_1\rho|h_{ss}|^2} \tag{10}$$

$$\gamma_{PU}^{(2)x_s} = \frac{a_2\rho\left|h_{sp}\right|^2}{1 + a_1\rho\left|h_{sp}\right|^2} \tag{11}$$

$$\gamma_{PU}^{(2)x_p} = \frac{a_1\rho\left|h_{sp}\right|^2}{1 + \beta a_2\rho\left|h_{sp}\right|^2} \tag{12}$$

$$\gamma_E^{(2)x_s} = \frac{a_2\rho|h_{se}|^2}{1 + \rho_j\left|h_{pe}\right|^2} \tag{13}$$

$$\gamma_E^{(2)x_p} = \frac{a_1\rho|h_{se}|^2}{1 + \rho_j\left|h_{pe}\right|^2} \tag{14}$$

where β ($0 \le \beta \le 1$) is the ipSIC parameter, $|h_{ss}|^2$, $\left|h_{sp}\right|^2$, $|h_{se}|^2$, and $\left|h_{pe}\right|^2$ are the channel gains between ST to SU, ST to PU, ST to Eve, and PT to Eve, respectively. The PU and Eve uses both SC/MRC techniques for processing the received signal, and then choose the data with the highest SNR from the two stages to demodulate. The PU and Eve rates corresponding to the two stages towards x_p and x_s can be denoted as [4], [5], [6], [7], [8], [9], [10], [11], [12], [13], [14], [15], [16], [17], [18], [19], [20], [21]:

$$\gamma_{PU}^{sc} = max(\gamma_{PU}^{(1)x_p}, \gamma_{PU}^{(2)x_p}) \tag{15}$$

$$\gamma_{PU}^{mrc} = \gamma_{PU}^{(1)x_p} + \gamma_{PU}^{(2)x_p} \tag{16}$$

$$\gamma_E^{sc} = \max\left(\gamma_E^{(1)x_p}, \gamma_E^{(2)x_p}\right) \tag{17}$$

$$\gamma_E^{mrc} = \gamma_E^{(1)x_p} + \gamma_E^{(2)x_p} \tag{18}$$

III. SECRECY PERFORMANCE ANALYSIS

A. SECRECY SUM RATE (SSR)

The secrecy sum rate (SSR) is obtained under two diversity techniques such as SC and MRC respectively, as follows:

$$R_{sum}^{\chi} = R_s^{PU(\chi)} + R_s^{SU} \tag{19}$$

where $\chi \in \{sc, mrc\}$.

$$R_s^{PU(sc)} = \frac{1}{2}log_2\left[\frac{1+\gamma_{PU}^{sc}}{1+\gamma_E^{sc}}\right]^+ \tag{20}$$

$$R_s^{PU(mrc)} = \frac{1}{2}log_2\left[\frac{1+\gamma_{PU}^{mrc}}{1+\gamma_E^{mrc}}\right]^+ \tag{21}$$

$$R_s^{SU} = \frac{1}{2}log_2\left[\frac{1+\gamma_{SU}^{(2)x_s}}{1+\gamma_E^{(2)x_s}}\right]^+ \tag{22}$$

where $[x]^+ = max(x, 0)$.

B. SECRECY OUTAGE PROBABILITY (SOP^{SA})

This part aims at how well the suggested overlay downlink CR-NOMA system using a single antenna works for SOP at two users, called PU and SU, in this way: The user's instantaneous SINR is less than a certain threshold, and the PU and SU signals (x_p and x_s) are sent at acceptable rates

(R_p and R_s). This leads to the outage. The proposed technique's SOP is stated as

1) SOP OF SECONDARY USER ($P_{X_S}^{SA}$)

The secondary user's SOP, i.e., $P_{x_s}^{SA}$, constitutes what preserves the secondary user through falling down if it correctly decodes the transmitted signal x_s that it received from x_{sc}. This is how the SOP of SU is described. and it is given by [21], [22], [23], [24], [25], and [26],

$$P_{x_s}^{SA} = \Pr(R_s^{SU} < R_s) \tag{23}$$

$$P_{x_s}^{SA} = \underbrace{\Pr\left(\frac{1+\gamma_{SU}^{x_s(2)}}{1+\gamma_E^{x_s(2)}} < 2^{2R_s}\right)}_{P_1} \tag{24}$$

where R_s is the target rate of symbol x_s and the secrecy outage of SU i.e., P_1 can be evaluated as follows:

$$\begin{aligned} P_1 &= \Pr\left(\gamma_{SU}^{x_s(2)} < 2^{2R_s}\gamma_E^{x_s(2)} + 2^{2R_s} - 1\right) \\ &= \int_0^\infty F_{\gamma_{SU}^{x_s(2)}}\left(2^{2R_s}\gamma + 2^{2R_s} - 1\right) f_{\gamma_E^{x_s(2)}}(\gamma)\, d\gamma \end{aligned} \tag{25}$$

$$\begin{aligned} P_1 &= \Pr\left(\gamma_{SU}^{x_s(2)} < 2^{2R_s}\gamma_E^{x_s(2)} + 2^{2R_s} - 1\right) \\ &= \int_0^\infty F_{\gamma_{SU}^{x_s(2)}}\left(2^{2R_s}\gamma + 2^{2R_s} - 1\right) f_{\gamma_E^{x_s(2)}}(\gamma)\, d\gamma \\ &= \int_0^\infty F_{\gamma_{SU}^{x_s(2)}}(\chi_s(\gamma)) f_{\gamma_E^{x_s(2)}}(\gamma)\, d\gamma \end{aligned} \tag{26}$$

where $\chi_s(\gamma) = 2^{2R_s}\gamma + 2^{2R_s} - 1$, the cumulative distribution function (CDF) and the probability density function (PDF) of SU and Eve during second transmission phase is $F_{\gamma_{SU}^{x_s(2)}}(\chi_s(\gamma)) = \Pr\left(\gamma_{SU}^{x_s(2)} < \chi_s(\gamma)\right)$, $f_{\gamma_E^{x_s(2)}}(\gamma) = \frac{d}{d\gamma} F_{\gamma_E^{x_s(2)}}(\gamma)$ and they can be derived as,

$$\begin{aligned} F_{\gamma_{SU}^{x_s(2)}}(\chi_s(\gamma)) &= \Pr\left(|h_{ss}|^2 < \frac{\chi_s(\gamma)}{(a_2 - a_1\chi_s(\gamma))\rho}\right) \\ &= 1 - \exp\left\{-\frac{\chi_s(\gamma)}{(a_2 - a_1\chi_s(\gamma))\lambda_{ss}\rho}\right\} \\ &= 1 - g_1(\chi_s(\gamma)) \end{aligned} \tag{27}$$

$$\begin{aligned} F_{\gamma_E}^{x_s(2)}(\gamma) &= \Pr\left(|h_{se}|^2 < \frac{\gamma\left(1+\rho_j|h_{pe}|^2\right)}{a_2\rho_E}\right) \\ &= \int_0^\infty \left(1 - F_{|h_{se}|^2}\left(\frac{\gamma\left(1+\rho_j x\right)}{a_2\rho_E}\right)\right) f_{|h_{pe}|^2}(x)\, dx \\ &= 1 - \frac{A\exp\{-K\gamma\}}{(A+\gamma)} \end{aligned} \tag{28}$$

where $A = \frac{a_2\rho_E\lambda_{se}}{\rho_j\lambda_{pe}}$, and $K = \frac{1}{a_2\rho_E\lambda_{se}}$. The PDF $f_{\gamma_E}^{x_s(2)}(\gamma)$ is obtained after applying derivative to the (28) as,

$$f_{\gamma_E}^{x_s(2)}(\gamma) = Ae^{-\gamma K}\left[\frac{K}{(A+\gamma)} + \frac{1}{(A+\gamma)^2}\right] \tag{29}$$

Hence, (26) can be rewritten using (27) and (29) as,

$$\begin{aligned} P_1 &= \int_0^\infty (1 - g_1(\chi_s(\gamma)))f_{\gamma_E^{x_s(2)}}(\gamma)\, d\gamma \\ &= 1 - \int_0^\infty f(\gamma) d\gamma \end{aligned} \tag{30}$$

where $f(\gamma) = g_1(\chi_s(\gamma))f_{\gamma_E^{x_s(2)}}(\gamma)$.

It's challenging to determine the integral in P_1. Gauss-Chebyshev quadrature is a way to compute that can be employed to find the proper results. After that, we can rewrite P_1 as [4], [21]:

$$P_1 = 1 - \frac{a\pi}{2n}\sum_{k=0}^{n-1}\sqrt{1-\theta_k^2} f\left(\frac{a}{2}\theta_k + \frac{a}{2}\right) \tag{31}$$

where $\theta_k = \cos\left(\frac{2k-1}{2n}\pi\right)$, a is sufficiently big number, the total number of Gauss-Chebyshev terminals is denoted as n.

2) SOP OF PRIMARY USER ($P_{X_P}^{SA}$)

The SOP of PU could have been written in such way that it is provided in [21], [22], [23], [24], [25], and [26], it is an outage event of PU that has not occurred once it is able to decode the signals x_s and x_p which were correctly received through PT/ST, respectively.

$$\begin{aligned} P_{x_p}^{SA} &= \Pr(R_s^{SU} < R_s, R_s^{PU} < R_p) \\ &\quad + \Pr(R_s^{SU} > R_s, R_s^{PU} < R_p) \end{aligned} \tag{32}$$

where the SOP of PU can be classified under two cases: 1) SC case, 2) MRC case as follows:

$$\begin{aligned} P_{x_p}^{SA} &= \underbrace{\Pr\left(\frac{1+\gamma_{SU}^{x_s(2)}}{1+\gamma_E^{x_s(2)}} < 2^{2R_s}\right)}_{P_1}\underbrace{\Pr\left(\frac{1+\gamma_{PU}^{\chi}}{1+\gamma_{Ep}^{\chi}} < 2^{2R_p}\right)}_{P_2^{\chi}} \\ &\quad + \left(1 - \underbrace{\Pr\left(\frac{1+\gamma_{SU}^{x_s(2)}}{1+\gamma_E^{x_s(2)}} < 2^{2R_s}\right)}_{P_1}\right) \\ &\quad \underbrace{\Pr\left(\frac{1+\gamma_{PU}^{\chi}}{1+\gamma_E^{\chi}} < 2^{2R_p}\right)}_{P_2^{\chi}} \end{aligned} \tag{33}$$

where $\chi \in \{sc, mrc\}$, R_p is the target rate of symbol x_p, and the secrecy outages P_1 (already evaluated and solution given in (31), and now P_2^{sc} & P_2^{mrc} can be derived as follows:

Case-1: SC Diversity

$$\begin{aligned} P_2^{sc} &= \Pr\left(\frac{1+\gamma_{PU}^{sc}}{1+\gamma_E^{sc}} < 2^{2R_p}\right) \\ &= \Pr\left(\gamma_{PU}^{sc} < 2^{2R_p}\gamma_E^{sc} + 2^{2R_p} - 1\right) \\ &= \int_0^{\infty} F_{\gamma_{PU}^{sc}}\left(2^{2R_p}\gamma + 2^{2R_p} - 1\right) f_{\gamma_E^{sc}}(\gamma)\, d\gamma \\ &= \int_0^{\infty} F_{\gamma_{PU}^{sc}}\left(\chi_p(\gamma)\right) f_{\gamma_E^{sc}}(\gamma)\, d\gamma \end{aligned} \tag{34}$$

where $\chi_p(\gamma) = 2^{2R_p}\gamma + 2^{2R_p} - 1$, the above CDF is function of $\chi_p(\gamma)$. According to the network model, the channel gains $|h_{pp}|^2$, $|h_{ps}|^2$, and $|h_{sp}|^2$ follows exponential distribution then their CDFs can be respectively, derived as,

$$\begin{aligned} F_{\gamma_{PU}^{sc}}\left(\chi_p(\gamma)\right) &= \Pr\left(\max\left(\gamma_{PU}^{(1)x_p}, \gamma_{PU}^{(2)x_p}\right) < \chi_p(\gamma)\right) \\ F_{\gamma_{PU}^{sc}}\left(\chi_p(\gamma)\right) &= 1 - \Pr\left(\max\left(\gamma_{PU}^{(1)x_p}, \gamma_{PU}^{(2)x_p}\right) > \chi_p(\gamma)\right) \\ F_{\gamma_{PU}^{sc}}\left(\chi_p(\gamma)\right) &= 1 - e^{-\left(\frac{\chi_p(\gamma)}{\lambda_{pp}\rho}\right)} e^{-\left(\frac{\chi_p(\gamma)}{(a_1 - a_2\gamma)\lambda_{sp}\rho}\right)} \\ F_{\gamma_{PU}^{sc}}\left(\chi_p(\gamma)\right) &= 1 - g_2\left(\chi_p(\gamma)\right) \end{aligned} \tag{35}$$

where the diversity PDF of Eve i.e., γ_E^{sc} during both first and second phases is a function of γ and it can be derived in proposition 1 & 2 (see the **Appendix. A**). Hence, (34) can be rewritten using (35) and (117) as,

$$\begin{aligned} P_2^{sc} &= \int_0^{\infty} \left(1 - g_2\left(\chi_p(\gamma)\right)\right) f_{\gamma_E^{sc}}(\gamma)\, d\gamma \\ &= 1 - \int_0^{\infty} f(\gamma) d\gamma \end{aligned} \tag{36}$$

where $f(\gamma) = g_2\left(\chi_p(\gamma)\right) f_{\gamma_E^{sc}}(\gamma)$.

Case-2: MRC Diversity

$$\begin{aligned} P_2^{mrc} &= \Pr\left(\frac{1+\gamma_{PU}^{mrc}}{1+\gamma_E^{mrc}} < 2^{2R_p}\right) \\ &= \Pr\left(\gamma_{PU}^{mrc} < 2^{2R_p}\gamma_E^{mrc} + 2^{2R_p} - 1\right) \\ &= \int_0^{\infty} F_{\gamma_{PU}^{mrc}}\left(2^{2R_p}\gamma + 2^{2R_p} - 1\right) f_{\gamma_E^{mrc}}(\gamma)\, d\gamma \\ &= \int_0^{\infty} F_{\gamma_{PU}^{mrc}}\left(\chi_p(\gamma)\right) f_{\gamma_E^{mrc}}(\gamma)\, d\gamma \end{aligned} \tag{37}$$

Let $y = \frac{a_1\rho|h_{sp}|^2}{1+\beta a_2\rho|h_{sp}|^2}$, where $y \in \{0, \omega\}$ with $\omega = \{\left(\chi_p(\gamma)\right), \frac{a_1}{\beta a_2}\}$. Similar to (35) the CDF under MRC diversity can be respectively, derived as [4],

$$\begin{aligned} F_{\gamma_{PU}^{mrc}}\left(\chi_p(\gamma)\right) &= \Pr\left(\gamma_{PU}^{(1)x_p} + \gamma_{PU}^{(2)x_p} < \chi_p(\gamma)\right) \\ &= \int_0^{\omega} \Pr\left(|h_{pp}|^2 < \frac{\chi_p(\gamma) - y}{\rho}\right) f_Y(y)\, dy \\ &= \int_0^{\omega} \left(1 - \exp\left\{-\frac{\chi_p(\gamma) - y}{\rho\lambda_{pp}}\right\}\right) f_Y(y)\, dy \\ &= F_Y(\omega) - \underbrace{\int_0^{\omega} \exp\left\{-\frac{\chi_p(\gamma) - y}{\rho\lambda_{pp}}\right\} f_Y(y)\, dy}_{P_A} \end{aligned} \tag{38}$$

where $f_Y(y)$ is the PDF of y. According to the probability theory [22], we can obtain $f_Y(y)$ and $F_Y(\omega)$ as,

$$f_Y(y) = \frac{a_1}{\rho\lambda_{sp}(a_1 - \beta a_2 y)^2} e^{\left\{-\frac{y}{\rho\lambda_{sp}(a_1 - \beta a_2 y)}\right\}} \tag{39}$$

$$F_Y(\omega) = \begin{cases} 1 - e^{\left\{-\frac{\chi_p(\gamma)}{\rho\lambda_{sp}\left(a_1 - \beta a_2 \chi_p(\gamma)\right)}\right\}} & \frac{a_1}{\beta a_2} \geq \chi_p(\gamma) \\ 1, & \frac{a_1}{\beta a_2} < \chi_p(\gamma) \end{cases} \tag{40}$$

To obtain an expression of P_A, we can substitute $f_Y(y)$ into the second term of (38). The closed form of P_A can be difficult to derive from immediate integration, though. By changing the value of $x = a_1 - \beta a_2 y$ and substituting $f_Y(y)$ into the second term of (38) we could rewrite P_A as,

$$P_A = \Lambda_1 \underbrace{\int_{a_1 - \beta a_2\omega}^{a_1} f(x)\, dx}_{P_B} \tag{41}$$

where $f(x) = \frac{1}{x^2}\exp\left\{-\frac{x}{\beta a_2\rho\lambda_{pp}} - \frac{a_1}{\beta a_2\rho\lambda_{pp}x}\right\}$, and $\Lambda_1 = \frac{a_1}{\beta a_2\rho\lambda_{pp}} e^{\frac{1}{\beta a_2\rho\lambda_{pp}} + \frac{a_1}{\beta a_2\rho\lambda_{pp}} - \frac{\chi_p(\gamma)}{\rho\lambda_{pp}}}$.

Here, we're going to show the closed-form equation of P_B applying the Gauss-Chebyshev quadrature technique [23].

$$P_B = \frac{\beta a_2\omega\pi}{2n} \sum_{k=1}^{n} \sqrt{1 - \theta_k^2} f\left(\frac{\beta a_2\omega}{2}\theta_k + \frac{\beta a_2\omega}{2}\right) \tag{42}$$

where the diversity PDF of Eve i.e., γ_E^{mrc} during both first and second phases is a function of γ and it can be derived in proposition 3 (see the **Appendix. A**).

Hence, (37) can be rewritten using (38), and (120) as,

$$\begin{aligned} P_2^{mrc} &= \int_0^{\infty} \left(1 - g_3\left(\chi_p(\gamma)\right)\right) f_{\gamma_E^{mrc}}(\gamma)\, d\gamma \\ &= 1 - \int_0^{\infty} f(\gamma) d\gamma \end{aligned} \tag{43}$$

where $f(\gamma) = g_3(\chi_p(\gamma)) f_{\gamma_E^{mrc}}(\gamma)$, and $g_3(\chi_p(\gamma)) = F_Y(\omega) - P_A$.

It's challenging to determine the integral in (36) & (44). Gauss-Chebyshev quadrature is a way to compute that can be employed to find the proper results. After that, we can rewrite (36) & (44) as [4], [21]:

$$P_2^{\chi} = 1 - \frac{a\pi}{2n} \sum_{k=0}^{n-1} \sqrt{1-\theta_k^2} f\left(\frac{a}{2}\theta_k + \frac{a}{2}\right) \tag{44}$$

where $\chi \in \{sc, mrc\}$.

Let $X \triangleq \frac{a_2\rho|h_{ss}|^2}{1+a_1\rho|h_{ss}|^2} \triangleq \frac{b|h_{ss}|^2}{1+a|h_{ss}|^2}$, where $a = a_1\rho$, $b = a_2\rho$, and similarly, let $Y \triangleq \frac{a_2\rho|h_{se}|^2}{1+\rho_j|h_{pe}|^2}$ and these two random variables X & Y follows exponential distribution, its PDF & CDFs can be respectively, given as,

$$f_{|h_{ss}|^2}(x) = \frac{1}{\lambda_{ss}} e^{-\frac{x}{\lambda_{ss}}} \tag{45}$$

$$F_Y(y) = 1 - \left(\frac{k_3}{k_3+y}\right) e^{-\frac{y}{\rho_E\lambda_{pe}}} \tag{46}$$

where $k_3 = \frac{\rho_2\lambda_{se}}{\rho_j\lambda_{pe}}$.

C. STRICTLY POSITIVE SECRECY CAPACITY ($SPSC^{SA}$)

SPSC is one of the most important performance measures for PLS. It shows the probability that exists information can be kept. So, it is easy to figure out the SPSC of our proposed overlay downlink CR-NOMA system as [24],

1) SPSC OF SECONDARY USER ($SPSC_{X_S}^{SA}$)

SPSC of SU can be expressed as,

$$SPSC_{x_s}^{SA} = Pr(R_s^{SU^{SA}} > 0) = \Pr\left(\gamma_{SU}^{x_s(2)} > \gamma_E^{x_s(2)}\right) = 1 - \underbrace{\Pr\left(\gamma_{SU}^{x_s(2)} < \gamma_E^{x_s(2)}\right)}_{P_3} \tag{47}$$

where IP of SU i.e., P_3 can be evaluated as follows:

$$P_3 = \int_0^{\infty} F_{\gamma_{SU}^{x_s(2)}}(\gamma) f_{\gamma_E^{x_s(2)}}(\gamma)\, d\gamma \tag{48}$$

where $F_{\gamma_{SU}^{x_s(2)}}(\gamma) = \Pr\left(\gamma_{SU}^{x_s(2)} < \gamma\right)$, $f_{\gamma_E^{x_s(2)}}(\gamma) = \frac{d}{d\gamma} F_{\gamma_E^{x_s(2)}}(\gamma)$ and they were already calculated and provided from (27) and (29) (for better understanding simply replace $\chi_s(\gamma)$ by γ), respectively.

Hence, (48) can be rewritten as,

$$P_3 = \int_0^{\infty} (1 - g_1(\gamma)) f_{\gamma_E^{x_s(2)}}(\gamma)\, d\gamma = 1 - \int_0^{\infty} g(\gamma) d\gamma \tag{49}$$

where $g(\gamma) = g_1(\gamma) f_{\gamma_E^{x_s(2)}}(\gamma)$.

It's challenging to determine the integral in P_3. Gauss-Chebyshev quadrature is a way to compute that can be employed to find the proper results. After that, we can rewrite P_3 as [4], [21]:

$$P_3 = 1 - \frac{a\pi}{2n} \sum_{i=0}^{n-1} \sqrt{1-\theta_i^2} g\left(\frac{a}{2}\theta_i + \frac{a}{2}\right) \tag{50}$$

where $\theta_i = \cos\left(\frac{2i-1}{2n}\pi\right)$, a is sufficiently big number, the total number of Gauss-Chebyshev terminals is denoted as n.

2) SPSC OF PRIMARY USER ($SPSC_{X_p}^{SA}$)

SPSC of PU can be expressed as,

$$SPSC_{x_p}^{SA} = Pr(R_s^{PU^{SA}} < 0, R_s^{SU^{SA}} < 0) + Pr(R_s^{PU^{SA}} < 0, R_s^{SU^{SA}} > 0) \tag{51}$$

where the SPSC of PU can be classified under two cases: 1) SC case, 2) MRC case as follows:

$$SPSC_{x_p}^{SA} = \underbrace{\Pr\left(\gamma_{PU}^{\chi} < \gamma_E^{\chi}\right)}_{P_4^{\chi}} \underbrace{\Pr\left(\gamma_{SU}^{x_s(2)} < \gamma_E^{x_s(2)}\right)}_{P_3} + \underbrace{\Pr\left(\gamma_{PU}^{\chi} < \gamma_E^{\chi}\right)}_{P_4^{\chi}} \left(1 - \underbrace{\Pr\left(\gamma_{SU}^{x_s(2)} < \gamma_E^{x_s(2)}\right)}_{P_3}\right) \tag{52}$$

where $\chi \in \{sc, mrc\}$, SPSC of SU i.e., P_3 (already evaluated and solution given in (50), and now SPSC of PU under SC/MRC cases i.e., P_4^{sc}/P_4^{mrc} can be evaluated as follows:

Case-1: SC Diversity

$$P_4^{sc} = \Pr\left(\gamma_{PU}^{sc} < \gamma_E^{sc}\right) = \int_0^{\infty} F_{\gamma_{PU}^{sc}}(\gamma) f_{\gamma_E^{sc}}(\gamma)\, d\gamma \tag{53}$$

where $F_{\gamma_{PU}^{sc}}(\gamma) = \Pr\left\{\max\left(\gamma_{PU}^{(1)x_p}, \gamma_{PU}^{(2)x_p}\right) < \gamma\right\}$, $f_{\gamma_E^{sc}}(\gamma) = \frac{d}{d\gamma} F_{\gamma_E^{sc}}(\gamma)$ and they were already calculated and provided from (29) & (33) (for better understanding simply replace $\chi_s(\gamma)$ by γ), respectively.

Hence, (53) can be rewritten as,

$$P_4^{sc} = \int_0^{\infty} (1 - g_2(\gamma)) f_{\gamma_E^{sc}}(\gamma)\, d\gamma = 1 - \int_0^{\infty} g(\gamma) d\gamma \tag{54}$$

where $g(\gamma) = g_2(\gamma) f_{\gamma_E^{sc}}(\gamma)$.

Case-2: MRC Diversity

$$P_4^{mrc} = \Pr\left(\gamma_{PU}^{mrc} < \gamma_E^{mrc}\right) = \int_0^{\infty} F_{\gamma_{PU}^{mrc}}(\gamma) f_{\gamma_E^{mrc}}(\gamma)\, d\gamma \tag{55}$$

where $F_{\gamma_{PU}^{mrc}}(\gamma) = \Pr\left\{\max\left(\gamma_{PU}^{(1)x_p}, \gamma_{PU}^{(2)x_p}\right) < \gamma\right\}$, $f_{\gamma_E^{mrc}}(\gamma) = \frac{d}{d\gamma}F_{\gamma_E^{mrc}}(\gamma)$ and they were already calculated and provided from (39) & (110) (for better understanding simply replace $\chi_s(\gamma)$ by γ), respectively.

Hence, (56) can be rewritten as,

$$P_4^{mrc} = \int_0^\infty (1 - g_2(\gamma)) f_{\gamma_E^{mrc}}(\gamma)\, d\gamma = 1 - \int_0^\infty g(\gamma) d\gamma \tag{56}$$

where $g(\gamma) = g_3(\gamma) f_{\gamma_E^{mrc}}(\gamma)$, $g_3(\gamma) = F_Y(\omega) - P_A$.

It's challenging to determine the integral in (55) & (57). Gauss-Chebyshev quadrature is a way to compute that can be employed to find the proper results. After that, we can rewrite (55) & (57) as [4], [21]:

$$P_4^X = 1 - \frac{a\pi}{2n}\sum_{i=0}^{n-1}\sqrt{1-\theta_i^2}\, g\left(\frac{a}{2}\theta_i + \frac{a}{2}\right) \tag{57}$$

where $X \in \{sc, mrc\}$.

Let $X \triangleq \rho|h_{pp}|^2$, $Y \triangleq \frac{a_1\rho|h_{sp}|^2}{1+\zeta a_2\rho|h_{sp}|^2}$, $U \triangleq \frac{\rho_E|h_{pe}|^2}{1+\rho_j|h_{sue}|^2}$, $V \triangleq \frac{a_1\rho|h_{se}|^2}{1+\rho_j|h_{pe}|^2}$, $Z = max(X, Y)$, and $W = max(U, V)$ and the CDF of Z/W can be respectively, derived as [29] and the CDFs of X, Y, U, and V can be derived, respectively as follows:

$$F_Z(z) = 1 - e^{-pz} \tag{58}$$

$$F_W(w) = 1 - \frac{A_1}{A_1 + z}\frac{A_2}{A_2 + z}e^{-mw} \tag{59}$$

where $p = \frac{1}{\rho\lambda_{pp}} + \frac{1}{\rho a_1\lambda_{sp}}$, $A_1 = \frac{\rho_E\lambda_{pe}}{\rho_j\lambda_{sue}}$, $A_2 = \frac{\rho_1\lambda_{se}}{\rho_j\lambda_{pe}}$, $m = \frac{1}{a_2\rho_E\lambda_{se}} + \frac{1}{\rho a_1\lambda_{se}}$, and assuming $\beta = 0$ for convenance.

D. AVERAGE SECRECY RATE (ASR^{SA})

Average secrecy rate is referred as the maximum achievable rate averaged over any fading channels. Here, we derive the closed-form solutions for the exact ASR under SA system for both PU and SU can be derived as follows:

1) ASR OF *PU* ($\bar{R}_S^{PU^{SA}}$)

$$\bar{R}_s^{PU^{SA}} = \frac{1}{2}\left[\int_0^\infty \log_2(1+z) f_Z(z) dz\right] - \frac{1}{2}\left[\int_0^\infty \log_2(1+w) f_W(w) dw\right] \tag{60}$$

Below proof is given in [26],

$$\int_0^\infty \log_2(1+x) f_X(x)\, dx = \frac{1}{\ln 2}\int_0^\infty \frac{1 - F_X(x)}{1+x} dx \tag{61}$$

$$\bar{R}_s^{PU^{SA}} = \frac{1}{2\ln 2}\int_0^\infty \frac{e^{-pz}}{1+z} dz - \frac{1}{\ln 2}\int_0^\infty \frac{\frac{A_1}{A_1+z}\frac{A_2}{A_2+z}e^{-mw}}{1+w} dw \tag{62}$$

Now the closed-form solution of (62) can be obtained using (58), (59), (61) and [27, (3.352.4)] as follows:

$$\bar{R}_s^{PU^{SA}} = \frac{-1}{2\ln 2}\left[-e^p Ei(-p)\right] + \chi_1\left[e^{mA_2}Ei(-mA_2) - e^m Ei(-m)\right] - \chi_1\left[e^{mA_2}Ei(-mA_2) - e^{A_1 m}Ei(-mA_1)\right] \tag{63}$$

where $\chi_1 = \frac{A_1A_2}{2\ln 2(A_1-1)(A_2-1)}$.

Let $X \triangleq \frac{a_2\rho|h_{ss}|^2}{1+a_1\rho|h_{ss}|^2} \triangleq \frac{b|h_{ss}|^2}{1+a|h_{ss}|^2}$, where $a = a_1\rho$, $b = a_2\rho$, and similarly, let $Y \triangleq \frac{a_2\rho|h_{se}|^2}{1+\rho_j|h_{pe}|^2}$ and where random variables X/Y follows exponential distribution, its PDF/CDFs can be respectively, given as,

$$f_{|h_{ss}|^2}(x) = \frac{1}{\lambda_{ss}}e^{-\frac{x}{\lambda_{ss}}} \tag{64}$$

$$F_Y(y) = 1 - \left(\frac{k_3}{k_3 + y}\right)e^{-\frac{y}{\rho_E\lambda_{pe}}} \tag{65}$$

where $k_3 = \frac{\rho_2\lambda_{se}}{\rho_j\lambda_{pe}}$.

2) ASR OF *SU* ($\bar{R}_S^{SU^{SA}}$)

$$\bar{R}_s^{SU^{SA}} = \frac{1}{2\ln 2}\int_0^\infty \ln\left(1 + \frac{bx}{1+ax}\right) f_{|h_{ss}|^2}(x)\, dx - \frac{1}{2}\int_0^\infty \log_2(1+y) f_Y(y)\, dy = \frac{1}{2\ln 2}\int_0^\infty \frac{1 - F_Y(y)}{1+y} dy \tag{66}$$

Following certain mathematical changes, (66) can be predicted by applying [27, (3.352.4) & (4.337.2)] as follows:

$$\bar{R}_s^{SU^{SA}} = \frac{1}{2\ln 2}e^{\frac{1}{a\lambda_{ss}}}Ei\left(\frac{-1}{a\lambda_{ss}}\right) \times \frac{1}{2\ln 2} - e^{\frac{1}{(a+b)\lambda_{ss}}}Ei\left(\frac{-1}{(a+b)\lambda_{ss}}\right) - \frac{k_3}{2\ln 2\,(k_3-1)}e^{\frac{1}{k_3\rho_2\lambda_{pe}}}Ei\left(\frac{-1}{k_3\rho_2\lambda_{pe}}\right) - \frac{k_3}{2\ln 2\,(k_3-1)}e^{\frac{1}{\rho_2\lambda_{pe}}}Ei\left(\frac{-1}{\rho_2\lambda_{pe}}\right) \tag{67}$$

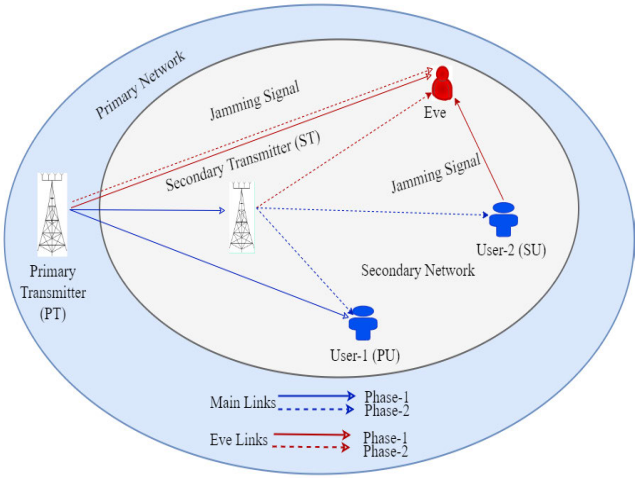

FIGURE 2. Proposed network model with multiple antennas (MA) case.

E. AVERAGE SECRECY SUM RATE ($ASSR^{SA}$)

From (63) and (67), the average secrecy sum rate under SA of the two users could be computed as,

$$ASSR^{SA} = \bar{R}_s^{PU^{SA}} + \bar{R}_s^{SU^{SA}} \tag{68}$$

IV. EXTENSION WITH MULTIPLE TRANSMIT ANTENNAS

Let us deal with a downlink overlay CR-NOMA architecture, depicted in Fig 2. The network consists of an array of M antennas at the primary transmitter (PT), an array of N antennas at the ST, two single-antenna users representing the PU and the SU, and a passive single-antenna eavesdropper referred to as Eve. All nodes are operating in HD mode for communication. Considering that the eavesdropper continues to overhear repeatedly. We presume the fact that all channels are independent, but all channels are not necessarily identically distributed Rayleigh fading channels. These fading channel coefficients are represented by $h_{ij,X}$, $i \in \{s,p\}$, $j \in \{s,p,E\}$, $X \in \{M,N\}$ which is modeled as an independent CSGD random variable with mean zero and variance $\lambda_{ij,X}$. Correspondingly, the channel gain $h_{ij,X}$ follows an exponential distribution with $\frac{1}{\lambda_{ij,X}}$. Let $|h_{ps,M}|^2$, $|h_{ss,N}|^2$, $|h_{pp,M}|^2$, and $|h_{sp,N}|^2$ are the channel gains between PT & ST, ST & SU, PT & PU, and ST & PU, with M, N, M, and N transmit antennas, respectively.

A. SECRECY OUTAGE PROBABILITY (SOP^{MA})

In this part, we analyze the performance of the suggested overlay CRN based downlink NOMA system equipped with multiple antennas (MA) using the secrecy outage probability (SOP) at two users i.e., PU, and SU, respectively as follows:

1) SOP OF SECONDARY USER ($P_{X_S}^{MA}$)

The SOP of secondary user i.e., $P_{x_s}^{MA}$, that is not in outage when it can decode the signal x_s successfully received from x_{sc}, the SOP of SU under MA based proposed CR-NOMA system can be expressed as [21], [22], [23], [24], [25], [26] and it is given as,

$$P_{x_s}^{MA} = Pr(R_s^{SU^{MA}} < R_s) \tag{69}$$

$$P_{x_s}^{MA} = \underbrace{\Pr\left(\frac{1+\gamma_{SU}^{x_s(2)}}{1+\gamma_E^{x_s(2)}} < 2^{2R_s}\right)}_{P_1^{MA}} \tag{70}$$

where R_s is the target rate of symbol x_s and the secrecy outage of SU i.e., P_1^{MA} can be evaluated as follows:

$$\begin{aligned} P_1^{MA} &= \Pr\left(\gamma_{SU}^{x_s(2)} < 2^{2R_s}\gamma_E^{x_s(2)} + 2^{2R_s} - 1\right) \\ &= \int_0^\infty F_{\gamma_{SU}^{x_s(2)}}\left(2^{2R_s}\gamma + 2^{2R_s} - 1\right) f_{\gamma_E^{x_s(2)}}(\gamma)\, d\gamma \\ &= \int_0^\infty F_{\gamma_{SU}^{x_s(2)}}(\chi_s(\gamma)) f_{\gamma_E^{x_s(2)}}(\gamma)\, d\gamma \end{aligned} \tag{71}$$

where $F_{\gamma_{SU}^{x_s(2)}}(\chi_s(\gamma)) = \Pr\left(\gamma_{SU}^{x_s(2)} < \chi_s(\gamma)\right)$, and $f_{\gamma_E^{x_s(2)}}(\gamma) = \frac{d}{d\gamma} F_{\gamma_E^{x_s(2)}}(\gamma)$. According to the network model shown in Fig. 2, $|h_{ss,N}|^2$ follows the Gamma distribution with $(N, \lambda_{ss,N})$ and the CDF can be calculated as,

$$\begin{aligned} F_{\gamma_{SU}^{x_s}}(\chi_s(\gamma)) &= \Pr\left(|h_{ss,N}|^2 < \frac{\chi_s(\gamma)}{(a_2 - a_1\chi_s(\gamma))\rho}\right) \\ &= 1 - \exp\left\{-\frac{\zeta_s(\gamma)}{\lambda_{ss,N}}\right\} \sum_{i=0}^{N-1} \frac{1}{i!}\left(\frac{\zeta_s(\gamma)}{\lambda_{ss,N}}\right)^i \\ &= 1 - g_1(\zeta_s(\gamma)) \end{aligned} \tag{72}$$

where $\zeta_s(\gamma) = \frac{\chi_s(\gamma)}{(a_2 - a_1\chi_s(\gamma))\rho}$.

Hence (71) can be modified using (72) and (29) as follows:

$$\begin{aligned} P_1^{MA} &= \int_0^\infty (1 - g_1(\zeta_s(\gamma))) f_{\gamma_E^{(2)x_s}}(\gamma)\, d\gamma \\ &= 1 - \int_0^\infty f(\gamma) d\gamma \end{aligned} \tag{73}$$

where $f(\gamma) = g_1(\zeta_s(\gamma)) f_{\gamma_E^{x_s}}(\gamma)$.

It's challenging to determine the integral in P_1^{MA}. Gauss-Chebyshev quadrature is a way to compute that can be employed to find the proper results. After that, we can rewrite P_1^{MA} as [4], [21]:

$$P_1^{MA} = 1 - \frac{a\pi}{2i} \sum_{k=0}^{n-1} \sqrt{1-\theta_k^2} f\left(\frac{a}{2}\theta_k + \frac{a}{2}\right) \tag{74}$$

2) SOP OF PRIMARY USER ($P_{X_P}^{MA}$)

The SOP of primary user i.e., $P_{x_p}^{MA}$, that is not in outage when it can decode the signal x_s, and x_p successfully received from PT/ST, the SOP of PU under MA based proposed CR-NOMA

system can be expressed as [21], [22], [23], [24], [25], [26] and it is given as,

$$P_{x_p}^{MA} = Pr(R_s^{PU^{MA}} < R_p, R_s^{SU^{MA}} < R_s) + Pr(R_s^{PU^{MA}} < R_p, R_s^{SU^{MA}} > R_s) \quad (75)$$

where the SOP of PU can be classified under two cases: 1) SC case, 2) MRC case as follows:

$$P_{x_p}^{MA} = \underbrace{\Pr\left(\frac{1+\gamma_{PU}^{\chi}}{1+\gamma_{Ep}^{\chi}} < 2^{2R_p}\right)}_{P_2{}^{MA-\chi}} \underbrace{\Pr\left(\frac{1+\gamma_{SU}^{x_s(2)}}{1+\gamma_{E}^{x_s(2)}} < 2^{2R_s}\right)}_{P_1{}^{MA}} + \underbrace{\Pr\left(\frac{1+\gamma_{PU}^{\chi}}{1+\gamma_{Ep}^{\chi}} < 2^{2R_p}\right)}_{P_2{}^{MA-\chi}} \left(1 - \underbrace{\Pr\left(\frac{1+\gamma_{SU}^{x_s(2)}}{1+\gamma_{E}^{x_s(2)}} < 2^{2R_s}\right)}_{P_1{}^{MA}}\right) \quad (76)$$

where R_p is the target rate of symbol x_p, and the secrecy outages P_1^{MA} (already evaluated and solution given in (74), and now P_2^{MA-sc} & P_2^{MA-mrc} can be evaluated as follows:

Case-1: SC Diversity

$$\begin{aligned} P_2^{MA-sc} &= \Pr\left(\frac{1+\gamma_{PU}^{sc}}{1+\gamma_{E}^{sc}} < 2^{2R_p}\right) \\ &= \Pr\left(\gamma_{PU}^{sc} < 2^{2R_p}\gamma_{E}^{sc} + 2^{2R_p} - 1\right) \\ &= \int_0^{\infty} F_{\gamma_{PU}^{sc}}\left(2^{2R_p}\gamma + 2^{2R_p} - 1\right) f_{\gamma_E^{sc}}(\gamma)\, d\gamma \\ &= \int_0^{\infty} F_{\gamma_{PU}^{sc}}\left(\chi_p(\gamma)\right) f_{\gamma_E^{sc}}(\gamma)\, d\gamma \end{aligned} \quad (77)$$

where the above CDF i.e., $F_{\gamma_{PU}^{sc}}\left(\chi_p(\gamma)\right)$ is function of $\chi_p(\gamma)$. According to our proposed system model shown in Fig. 2, $|h_{pp,M}|^2$, and $|h_{sp,N}|^2$, respectively, follows the Gamma distribution with parameters $(M, \lambda_{pp,M})$, $(N, \lambda_{sp,N})$ and the CDFs could be derived as,

$$\begin{aligned} F_{\gamma_{PU}^{(1)x_p}}\left(\chi_p(\gamma)\right) &= \Pr\left(|h_{pp,M}|^2 < \frac{\chi_p(\gamma)}{\rho}\right) \\ &= 1 - \exp\left\{-\frac{\chi_p(\gamma)}{\rho\lambda_{pp,M}}\right\} \sum_{i=0}^{M-1} \frac{1}{i!}\left(\frac{\chi_p(\gamma)}{\rho\lambda_{pp,M}}\right)^i \\ &= 1 - g_2(\chi_p(\gamma)) \end{aligned} \quad (78)$$

$$\begin{aligned} F_{\gamma_{PU}^{(2)x_p}}\left(\chi_p(\gamma)\right) &= \Pr\left(|h_{sp,N}|^2 < \frac{\chi_p(\gamma)}{\rho}\right) \\ &= 1 - \exp\left\{-\frac{\zeta_p(\gamma)}{\lambda_{sp,N}}\right\} \sum_{i=0}^{N-1} \frac{1}{i!}\left(\frac{\zeta_p(\gamma)}{\lambda_{sp,N}}\right)^i \\ &= 1 - g_3(\zeta_p(\gamma)) \end{aligned} \quad (79)$$

where $\zeta_p(\gamma) = \frac{\chi_p(\gamma)}{(a_1 - \beta a_2 \chi_p(\gamma))\rho}$. Then, the overall CDF of γ_{PU} can be calculated as,

$$\begin{aligned} F_{\gamma_{PU}^{sc}}\left(\chi_p(\gamma)\right) &= \Pr\left(\gamma_{PU}^{sc} < \chi_p(\gamma)\right) \\ &= 1 - \Pr\left(\gamma_{PU}^{(1)x_p} > \chi_p(\gamma)\right) \Pr\left(\gamma_{PU}^{(2)x_p} > \chi_p(\gamma)\right) \\ &= 1 - g_2(\chi_p(\gamma)) g_3(\zeta_p(\gamma)) \end{aligned} \quad (80)$$

where the diversity PDF of Eve i.e., γ_E^{sc} during both first and second phases is a function of γ and it can be derived in proposition 4 & 5 (see the **Appendix. B**). Hence, (77) can be rewritten using (80), and (117) as,

$$\begin{aligned} P_2^{MA-sc} &= \int_0^{\infty} \left(1 - g_2(\chi_p(\gamma)) g_3(\zeta_p(\gamma))\right) f_{\gamma_E^{sc}}(\gamma)\, d\gamma \\ &= 1 - \int_0^{\infty} f(\gamma) d\gamma \end{aligned} \quad (81)$$

where $f(\gamma) = g_2(\chi_p(\gamma)) g_3(\zeta_p(\gamma)) f_{\gamma_E^{sc}}(\gamma)$.

It's challenging to determine the integral in P_2^{MA-sc}. Gauss-Chebyshev quadrature is a way to compute that can be employed to find the proper results. After that, we can rewrite P_2^{MA-sc} as [4], [21]:

$$P_2^{MA-sc} = 1 - \frac{a\pi}{2i} \sum_{k=0}^{n-1} \sqrt{1-\theta_k^2} f\left(\frac{a}{2}\theta_k + \frac{a}{2}\right) \quad (82)$$

Case-2: MRC Diversity

$$\begin{aligned} P_2^{MA-mrc} &= \Pr\left(\frac{1+\gamma_{PU}^{mrc}}{1+\gamma_{E}^{mrc}} < 2^{2R_p}\right) \\ &= \Pr\left(\gamma_{PU}^{mrc} < 2^{2R_p}\gamma_{E}^{mrc} + 2^{2R_p} - 1\right) \\ &= \int_0^{\infty} F_{\gamma_{PU}^{mrc}}\left(2^{2R_p}\gamma + 2^{2R_p} - 1\right) f_{\gamma_E^{mrc}}(\gamma)\, d\gamma \\ &= \int_0^{\infty} F_{\gamma_{PU}^{mrc}}\left(\chi_p(\gamma)\right) f_{\gamma_E^{mrc}}(\gamma)\, d\gamma \end{aligned} \quad (83)$$

where the above CDF i.e., $F_{\gamma_{PU}^{mrc}}\left(\chi_p(\gamma)\right)$ is function of $\chi_p(\gamma)$. Let $y = \frac{a_1\rho|h_{sp,N}|^2}{1+\beta a_2\rho|h_{sp,N}|^2}$, where $y \in \{0, \omega\}$ with $\omega = \{\left(\chi_p(\gamma)\right), \frac{a_1}{\beta a_2}\}$. According to our proposed system model shown in Fig. 2, $|h_{pp,M}|^2$, and $|h_{sp,N}|^2$, respectively, follows the Gamma distribution with parameters $(M, \lambda_{pp,M})$, and $(N, \lambda_{sp,N})$, respectively. Similar to (38) the CDFs under MRC diversity can be respectively, derived as [4]:

$$\begin{aligned} F_{\gamma_{PU}^{mrc}}\left(\chi_p(\gamma)\right) &= \Pr\left(\gamma_{PU}^{(1)x_p} + \gamma_{PU}^{(2)x_p} < \chi_p(\gamma)\right) \\ &= \int_0^{\omega} \Pr\left(|h_{pp,M}|^2 < \frac{\chi_p(\gamma) - y}{\rho}\right) f_Y(y)\, dy \\ &= \int_0^{\omega} \left(1 - \exp\left\{-\frac{\chi_p(\gamma) - y}{\rho\lambda_{pp,M}}\right\}\right) f_Y(y)\, dy \end{aligned}$$

$$= F_Y(\omega) - \underbrace{\int_0^{\omega} \exp\left\{-\frac{\chi_p(\gamma) - y}{\rho\lambda_{pp,M}}\right\} f_Y(\gamma)\, dy}_{P_A} \tag{84}$$

where $f_Y(y)$ is the PDF of y. According to the probability theory [22], we can obtain $f_Y(y)$ and $F_Y(\omega)$ as,

$$f_Y(y) = \frac{a_1\left(\frac{y}{\rho\lambda_{sp,N}}\right)^{N-1}}{\rho\lambda_{sp,N}(a_1 - \beta a_2 y)^2 (N-1)!} \exp\left\{-\frac{y}{\rho\lambda_{sp,N}}\right\} \tag{85}$$

$$F_Y(\omega) = \begin{cases} 1 - e^{-\left(\frac{\zeta_p(\gamma)}{\lambda_{sp,N}}\right)} \sum_{i=0}^{N-1} \frac{1}{i!}\left(\frac{\zeta_p(\gamma)}{\lambda_{sp,N}}\right)^i & \frac{a_1}{\beta a_2} \geq \chi_p(\gamma) \\ 1, & \frac{a_1}{\beta a_2} < \chi_p(\gamma) \end{cases} \tag{86}$$

To obtain an expression of P_A, we can substitute $f_Y(y)$ into the second term of (83). The closed form of P_A can be difficult to derive from immediate integration, though. By changing the value of $x = a_1 - \beta a_2 y$ and substituting $f_Y(y)$ into the second term of (83) we could rewrite P_A as,

$$P_A = \Lambda_1 \underbrace{\int_{a_1 - \beta a_2 \omega}^{a_1} f(x)\, dx}_{P_B} \tag{87}$$

where $f(x) = \frac{(a_1 - x)^{N-1}}{x^2} \exp\left\{-\frac{x}{\beta a_2 \rho\lambda_{pp,M}} - \frac{a_1}{\beta a_2 \rho\lambda_{pp,M} x}\right\}$, and $\Lambda_1 = \frac{a_1}{\beta a_2 \rho\lambda_{pp,M}(N-1)!} e^{\frac{1}{\beta a_2 \rho\lambda_{pp,M}} + \frac{a_1}{\beta a_2 \rho\lambda_{pp,M}} - \frac{\chi_p(\gamma)}{\rho\lambda_{pp,M}}}$.

Here, we're going to show the closed-form equation of P_B applying the Gauss-Chebyshev quadrature technique [23].

$$P_B = \frac{\beta a_2 \omega \pi}{2n} \sum_{k=1}^{n} \sqrt{1 - \theta_k^2} f\left(\frac{\beta a_2 \omega}{2}\theta_k + \frac{\beta a_2 \omega}{2}\right) \tag{88}$$

where the diversity PDF of Eve i.e., γ_E^{mrc} during both first and second phases is a function of γ and it can be derived in proposition 3 (see the **Appendix. A**).

Hence, (83) can be rewritten using (84), and (120) as,

$$P_2^{MA-mrc} = \int_0^{\infty} \left(1 - g_2(\zeta_p(\gamma)) g_3(\zeta_p(\gamma))\right) f_{\gamma_E^{mrc}}(\gamma)\, d\gamma$$
$$= 1 - \int_0^{\infty} f(\gamma) d\gamma \tag{89}$$

where $f(\gamma) = g_2(\zeta_p(\gamma)) g_3(\zeta_p(\gamma)) f_{\gamma_E^{sc}}(\gamma)$.

It's challenging to determine the integral in P_2^{MA-mrc}. Gauss-Chebyshev quadrature is a way to compute that can be employed to find the proper results. After that, we can rewrite P_2^{MA-mrc} as [4], [21]:

$$P_2^{MA-mrc} = 1 - \frac{a\pi}{2i} \sum_{k=0}^{n-1} \sqrt{1 - \theta_k^2} f\left(\frac{a}{2}\theta_k + \frac{a}{2}\right) \tag{90}$$

B. STRICTLY POSITIVE SECRECY CAPACITY ($SPSC^{MA}$)

In this part, SPSC for the proposed overlay CR-NOMA system under MA scenario is estimated as follows:

1) SPSC OF SECONDARY USER ($SPSC_{X_S}^{MA}$)

The SPSC of SU under MA case can be expressed as,

$$SPSC_{x_s}^{MA} = Pr(R_s^{SU^{MA}} > 0) = \Pr\left(\gamma_{SU}^{x_s(2)} > \gamma_E^{x_s(2)}\right)$$
$$= 1 - \underbrace{\Pr\left(\gamma_{SU}^{x_s(2)} < \gamma_E^{x_s(2)}\right)}_{P_3^{MA}} \tag{91}$$

where SPSC of SU i.e., P_3^{MA} can be evaluated as follows:

$$P_3^{MA} = \int_0^{\infty} F_{\gamma_{SU}^{x_s(2)}}(\gamma) f_{\gamma_E^{x_s(2)}}(\gamma)\, d\gamma \tag{92}$$

where $F_{\gamma_{SU}^{x_s(2)}}(\gamma) = \Pr\left(\gamma_{SU}^{x_s(2)} < \gamma\right)$, $f_{\gamma_E^{x_s(2)}}(\gamma) = \frac{d}{d\gamma} F_{\gamma_E^{x_s(2)}}(\gamma)$ and they were already calculated and provided from (72) and (29) (for better understanding simply replace $\zeta_s(\gamma)$ by γ), respectively.

Hence, (92) can be rewritten as,

$$P_3^{MA} = \int_0^{\infty} (1 - g_1(\gamma)) f_{\gamma_E^{x_s(2)}}(\gamma)\, d\gamma$$
$$= 1 - \int_0^{\infty} g(\gamma) d\gamma \tag{93}$$

where $g(\gamma) = g_1(\gamma) f_{\gamma_E^{x_s(2)}}(\gamma)$.

It's challenging to determine the integral in P_3^{MA}. Gauss-Chebyshev quadrature is a way to compute that can be employed to find the proper results. After that, we can rewrite P_3^{MA} as [4], [21]:

$$P_3^{MA} = 1 - \frac{a\pi}{2n} \sum_{k=0}^{n-1} \sqrt{1 - \theta_k^2} f\left(\frac{a}{2}\theta_k + \frac{a}{2}\right) \tag{94}$$

2) SPSC OF PRIMARY USER ($SPSC_{X_P}^{MA}$)

The SPSC of PU can be expressed as,

$$SPSC_{x_p}^{MA} = Pr(R_s^{PU^{SA}} > 0, R_s^{SU^{SA}} > 0) \tag{95}$$

where the SPSC of PU can be classified under two cases: 1) SC case, 2) MRC case as follows:

$$SPSC_{x_p}^{MA} = \underbrace{\Pr\left(\gamma_{PU}^{\chi} > \gamma_E^{\chi}\right)}_{P_4^{MA-\chi}} \underbrace{\Pr\left(\gamma_{SU}^{x_s(2)} > \gamma_E^{x_s(2)}\right)}_{P_3^{MA}} \tag{96}$$

where the SPSC of SU i.e., P_3^{MA} (already evaluated and solution given in (94), and now SPSC of PU i.e., P_4^{MA-sc}/P_4^{MA-mrc} can be evaluated as follows:

Case-1: SC Diversity

$$P_4^{MA-sc} = \Pr\left(\gamma_{PU}^{sc} > \gamma_E^{sc}\right)$$
$$P_4^{MA-sc} = \int_0^\infty F_{\gamma_{PU}^{sc}}(\gamma) f_{\gamma_E^{sc}}(\gamma)\, d\gamma \tag{97}$$

where $F_{\gamma_{PU}^{sc}}(\gamma)$ & $f_{\gamma_E^{sc}}(\gamma)$ and they were already calculated and provided from (80) & (117) (for better understanding simply replace $\zeta_p(\gamma)$ by γ), respectively.

Hence, (96) can be rewritten as,

$$P_4^{MA-sc} = \int_0^\infty (1 - g_2(\gamma) g_3(\gamma)) f_{\gamma_E^{sc}}(\gamma)\, d\gamma$$
$$= 1 - \int_0^\infty g(\gamma) d\gamma \tag{98}$$

where $g(\gamma) = g_2(\gamma) g_3(\gamma) f_{\gamma_E^{sc}}(\gamma)$.

Case-2: MRC Diversity

$$P_4^{MA-mrc} = \Pr\left(\gamma_{PU}^{mrc} > \gamma_E^{mrc}\right)$$
$$P_4^{MA-mrc} = \int_0^\infty F_{\gamma_{PU}^{mrc}}(\gamma) f_{\gamma_E^{mrc}}(\gamma)\, d\gamma \tag{99}$$

where $F_{\gamma_{PU}^{mrc}}(\gamma)$ & $f_{\gamma_E^{mrc}}(\gamma)$ and they were already calculated and provided from (84) & (120) (for better understanding simply replace $\zeta_p(\gamma)$ by γ), respectively.

Hence, (99) can be rewritten as,

$$P_4^{MA-mrc} = \int_0^\infty (1 - g_2(\gamma) g_3(\gamma)) f_{\gamma_E^{mrc}}(\gamma)\, d\gamma$$
$$= 1 - \int_0^\infty g(\gamma) d\gamma \tag{100}$$

where $g(\gamma) = g_2(\gamma) g_3(\gamma) f_{\gamma_E^{mrc}}(\gamma)$.

It's challenging to determine the integral in P_4^{MA-sc} and P_4^{MA-mrc}. Gauss-Chebyshev quadrature is a way to compute that can be employed to find the proper results. After that, we can rewrite P_4^{MA-sc} and P_4^{MA-mrc} as [4], [21]:

$$P_4^{MA-\chi} = 1 - \frac{a\pi}{2n} \sum_{k=0}^{n-1} \sqrt{1-\theta_k^2}\, g\left(\frac{a}{2}\theta_k + \frac{a}{2}\right) \tag{101}$$

Let $X \triangleq \rho\left|h_{pp,M}\right|^2$, $Y \triangleq a_1\rho\left|h_{sp,N}\right|^2$, where $\left|h_{pp,M}\right|^2$, and $\left|h_{sp,N}\right|^2$ both follows Gamma distribution, and the CDFs of X, and Y are provided from (78), (79), respectively.

Similarly, let $U \triangleq \frac{\rho_E\left|h_{pe,M}\right|^2}{1+\rho_j\left|h_{sue}\right|^2}$, $V \triangleq \frac{a_1\rho\left|h_{se,N}\right|^2}{1+\rho_j\left|h_{pe}\right|^2}$, and the CDFs of U, and V are provided from (75), and (78), respectively. Let us define $Z = max(X, Y)$, and $W = max(U, V)$ and the combined CDFs of Z and W can be respectively, derived as [29],

$$F_Z(z) = 1 - e^{-K_1 z}\left(1 + \frac{z}{\rho\lambda_{pp}}\right)\left(1 + \frac{z}{\rho_1\lambda_{sp}}\right) \tag{102}$$

$$F_W(w) = 1 - \frac{\exp(\lambda_{1E} + \lambda_{2E}) K_2 K_3}{\left(w + \frac{1}{K_2}\right)^M \left(w + \frac{1}{K_3}\right)^N} \tag{103}$$

where $K_1 = \frac{1}{\rho\lambda_{pp,M}} + \frac{1}{\rho_1\lambda_{sp,N}}$,
$K_2 = \left(\lambda_{pe}\rho_E\lambda_{1E}\right)^M$,
$K_3 = \left(\lambda_{pe}\rho_E\lambda_{2E}\right)^N$.

C. AVERAGE SECRECY RATE (ASR^{MA})

Here, we derive the closed-form solutions for the exact ASR under MA case for both PU and SU can be derived as follows:

1) ASR OF PU ($\bar{R}_S^{PU^{MA}}$)

ASR of PU can be expressed as,

$$\bar{R}_s^{PU^{MA}} = \frac{1}{\ln 2}\int_0^\infty \frac{1 - F_Z(z)}{1+z} dz + \frac{1}{\ln 2}\int_0^\infty \frac{1 - F_W(w)}{1+w} dw \tag{104}$$

$$\bar{R}_s^{PU^{MA}} = \frac{1}{2\ln 2}\int_0^\infty \frac{e^{-K_1 z}\left(1 + \frac{z}{\rho\lambda_{pp}}\right)\left(1 + \frac{z}{\rho_1\lambda_{sp}}\right)}{1+z} dz$$
$$- \frac{\exp(\lambda_{1E}+\lambda_{2E}) K_2 K_3}{2\ln 2}\int_0^\infty \frac{(1+w)^{-1}}{\left(w+\frac{1}{K_3}\right)^M \left(w+\frac{1}{K_4}\right)^N} dw \tag{105}$$

Now the closed-form solution of (105) can be obtained using (102), (103), (104) and [27, (3.352.4)] as follows:

$$\bar{R}_s^{PU^{MA}} = \frac{-1}{2\ln 2}\left(e^{K_1} Ei(-K_1)\right)$$
$$+ \frac{1}{2\ln 2}\left(\frac{1}{K_1} + e^{K_1} Ei(-K_1)\right)$$
$$+ \frac{1}{2\ln 2}\left(\frac{1}{{K_1}^2} + \frac{1}{K_1} - e^{K_1} Ei(-K_1)\right)$$
$$+ \frac{\exp(\lambda_{1E}+\lambda_{2E}) K_2 K_3}{2\ln 2}\int_0^\infty \frac{(1+w)^{-1}}{\left(w+\frac{1}{K_3}\right)^M \left(w+\frac{1}{K_4}\right)^N} dw \tag{106}$$

Let $X \triangleq \frac{a_2\rho\left|h_{ss,N}\right|^2}{1+a_1\rho\left|h_{ss}\right|^2}$, $Y \triangleq \frac{a_2\rho\left|h_{se}\right|^2}{1+\rho_j\left|h_{pe,M}\right|^2}$ and where random variables $\left|h_{ss,N}\right|^2$, follows Gamma distribution and its CDFs can be respectively, given as,

$$F_X(x) = 1 - \exp\left\{-\frac{x}{\rho_2\lambda_{ss,N}}\right\}\sum_{i=0}^{N-1}\frac{1}{i!}\left(\frac{x}{\rho_2\lambda_{ss,N}}\right)^i$$
$$= 1 - \exp\left\{-\frac{x}{\rho_2\lambda_{ss,N}}\right\}\frac{x^{N-1}}{(N-1)!\left(\rho_2\lambda_{ss,N}\right)^{N-1}} \tag{107}$$

Now we follow the similar procedure as **proposition 2** to derive the CDF of Y as,

$$F_Y(y) = 1 - \frac{\exp(\lambda_{3E})}{(1+\lambda_{se}\rho_2\lambda_{3E}y)^M} = 1 - \frac{\exp(\lambda_{3E})}{\left(y+\frac{1}{K_4}\right)^M} \quad (108)$$

where $\lambda_{3E} = \frac{\lambda_{pe}}{a_2\rho}$, and $K_4 = (\lambda_{se}\rho_2\lambda_{3E})^M$.

2) ASR OF SU ($\bar{R}_S^{SU^{MA}}$)

The ASR of SU can be expressed as,

$$\bar{R}_s^{SU^{MA}} = \frac{1}{\ln 2}\int_0^\infty \frac{1-F_X(x)}{1+x}dx + \frac{1}{\ln 2}\int_0^\infty \frac{1-F_Y(y)}{1+y}dy \quad (109)$$

$$\bar{R}_s^{SU^{MA}} = \frac{1}{(N-1)!2\ln 2(\rho_2\lambda_{ss})^{N-1}}\int_0^\infty \frac{x^{N-1}e^{-\frac{x}{\rho_2\lambda_{ss}}}}{(1+x)}dx - \frac{K_4 e^{\lambda_{3E}}}{2\ln 2}\int_0^\infty \frac{(1+y)^{-1}}{\left(y+\frac{1}{K_4}\right)^M}dy \quad (110)$$

Following certain mathematical changes, (110) can be predicted by applying (107), (108), and [27, (3.353.5)] as follows:

$$\bar{R}_s^{SU^{MA}} = \frac{1}{(N-1)!2\ln 2(\rho_2\lambda_{ss})^{N-1}}\left[e^{\frac{1}{\rho_2\lambda_{ss}}}Ei\left(-\frac{1}{\rho_2\lambda_{ss}}\right)+\rho_2\lambda_{ss}\right] - \frac{K_4 e^{\lambda_{3E}}}{2\ln 2}\int_0^\infty \frac{(1+y)^{-1}}{\left(y+\frac{1}{K_4}\right)^M}dy \quad (111)$$

where, the integral parts in (106) & (111) is difficult to obtain a closed-form and as it can be simulated using MATLAB.

D. AVERAGE SECRECY SUM RATE ($ASSR^{MA}$)

From (106) and (111), the average secrecy sum rate of the two users could be computed as,

$$ASSR^{MA} = \bar{R}_s^{PU^{MA}} + \bar{R}_s^{SU^{MA}} \quad (112)$$

Remarks: As mentioned in the previous two sections, two single antenna users have distinct SOP, SPSC as well as ASR/ASSR, which is mostly determined by power allocation variables and channel gains. Multi-antenna transmitters, on the other hand, demonstrate improved SOP, SPSC as well as ASR/ASSR performance, as described in (54), (58) (67), (70), (79) and (84), respectively. In the context of an overlay CR-NOMA method, the downlink communication tasks exhibit more sophisticated representations of secure performance. Despite the fact that end-to-end SINR and target transmission rate are comparable, the criteria for selecting for two MA transmitting devices is an arrangement of the most effective antennas for transmitting information.

TABLE 2. Simulation parameters.

Parameter	Description	Value
M	Number of Transmit Antennas	2
N	Number of Transmit Antennas	2
W	Bandwidth	6MHz
a_1	PA Coefficient for PU	0.4
a_2	PA Coefficient for SU	0.6
α	Path Loss Exponent	4
ρ	Transmit SNR	0-40 dB
ζ	ipSIC Parameter	0.05-0.3

To maintain confidentiality in wireless channel, it is feasible to transmit both the information-bearing signal and the jamming signals simultaneously through several antennas at the transmitter. From the literature, it can be affirmed that different type of jamming signals can be employed. For instance, friendly jammer (FJ) signal was employed in [10], while, cooperative jamming signal was used in [21] and [26] and artificial-noise (AN) aided jamming signal was employed in [41], [42], and [43] for safeguarding the system's security aspects. The information signal becomes hidden during propagation by radiating the generated noise isotropically. Alike [10], in our work we have assumed that jamming signals are known at the intended users and when users receive the signal, they first detect the jamming signal, remove that signal, and then decode the information signal.

V. NUMERICAL AND SIMULATION RESULTS

In this section, the outcomes of both the analytical and simulation are shown in order to demonstrate that the suggested secured system is trustworthy. We get outcomes from simulations that have been determined on the assessment we did earlier. Let $R_p = 1$bit/s/Hz, $R_s = 0.5$bit/s/Hz, the noise power is $\sigma^2 = -110$dBm. As we set the distances between each varies from 100m to 1km. The Gauss-Chebyshev node is set to $n = 200$.

Fig 3, shows a performance comparison between the proposed overlay CR-NOMA system with and without jamming at the Eve in terms of the SOP of PU and SU versus transmit SNR, respectively. The results obtained under the system without jamming is shows that, the SOP of PU and SU is very close to unity, where the PIC scheme is implemented at Eve. Therefore, in the suggested approach, an artificial jamming signal is utilised to guarantee safe reception. Our investigation is confirmed by the conformance between the mathematical and the simulation outcomes for the suggested system. It is also clear that the proposed overlay CR-NOMA system with jamming improves over the without jamming schemes in terms of PU/SU's secrecy performances under pSIC/ipSIC. Since always strong user performs better than the weak user, the SOP performance of PU in the proposed

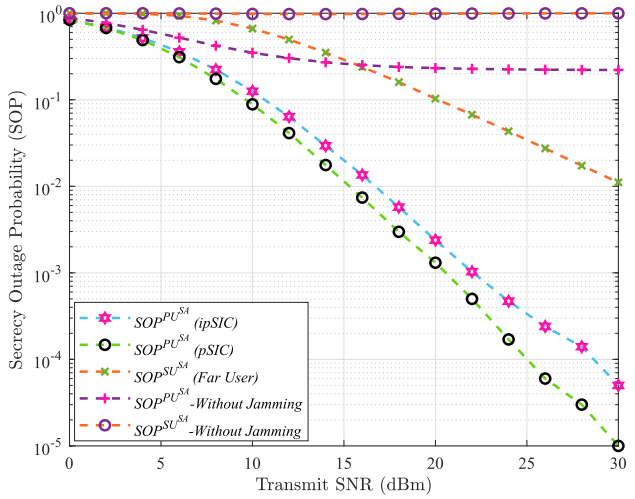

FIGURE 3. Transmit SNR Vs secrecy outage probability performance comparison between SA-based overlay CR-NOMA system and MA based overlay CR-NOMA system under both pSIC/ipSIC assumptions.

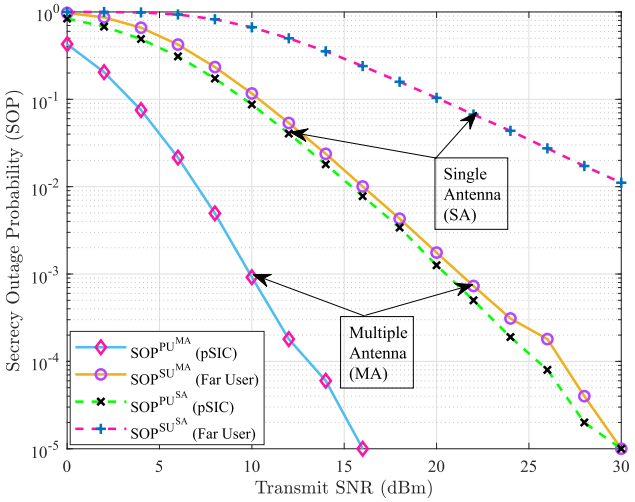

FIGURE 4. Transmit SNR Vs secrecy outage probability under both SA and MA Case(s).

NOMA scheme is higher than that of SU, as illustrated in Fig 3.

The secrecy performance comparison of our proposed overlay CR-NOMA system equipped with single and multiple antennas is simulated in Fig 4 under the presence of the Eve in terms of the SOP of PU and SU versus transmit SNR. The results obtained in Fig 4 clearly shows that under the influence of MA system our proposed system exhibits improved SOP performances of PU and SU than the system equipped with SA. Therefore, in the suggested approach with MA system, an artificial jamming signal is utilised to guarantee safe reception. Our investigation is confirmed by the conformance between the mathematical and the simulation outcomes for the suggested system.

The secrecy performance comparison in terms of SOP of PU and SU versus transmit SNR of our proposed overlay

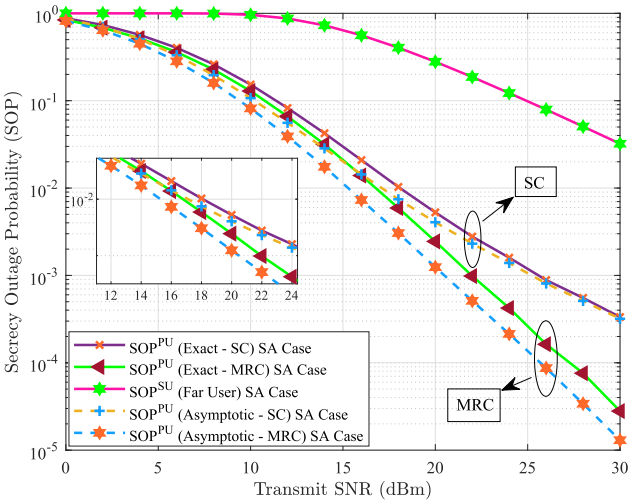

FIGURE 5. Performance comparison of SC and MRC diversity techniques in terms of Transmit SNR Vs Exact/Asymptotic SOP (under SA Case).

CR-NOMA system which is equipped with single and multiple antennas is simulated in Fig 4 under the presence of the Eve. From the simulation results obtained in Fig 4 clearly demonstrates that under the influence of MA system our proposed system exhibits improved SOP performances of PU and SU than the system equipped with SA. Therefore, in the suggested approach with MA system, an artificial jamming signal is utilised to guarantee safe reception. Our investigation is confirmed by the conformance between the mathematical and the simulation outcomes for the suggested system.

The secrecy performance comparison of our proposed overlay CR-NOMA system which is equipped with SA is simulated in Fig 5 under the presence of the Eve in terms of the SOP of PU and SU versus transmit SNR. The results obtained in Fig 5 clearly shows that under the influence of SC/MRC diversity techniques for processing the received signals at the PU/Eve end, our proposed system exhibits improved SOP performances of PU under MRC scheme than the system equipped with SC technique. Moreover, the asymptotic behavior outperforms the exact SNR behaviors under both SC/MRC techniques. Therefore, in the suggested approach with SA system, an artificial jamming signal is utilised to guarantee safe reception. Our investigation is confirmed by the conformance between the mathematical and the simulation outcomes for the suggested system.

The secrecy performance comparison of our proposed overlay CR-NOMA system equipped with MA is simulated in Fig 6 under the presence of the Eve in terms of the SOP of PU and SU versus transmit SNR. The results obtained in Fig 6 clearly shows that under the influence of SC/MRC diversity techniques for processing the received signals at the PU/Eve end, our proposed system exhibits improved SOP performances of PU under MRC than the system equipped with SC method.

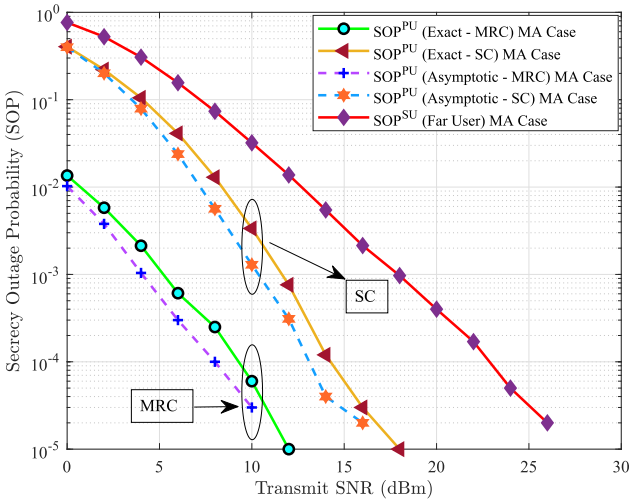

FIGURE 6. Performance comparison of SC and MRC diversity techniques in terms of Transmit SNR Vs Exact/Asymptotic SOP (under MA Case).

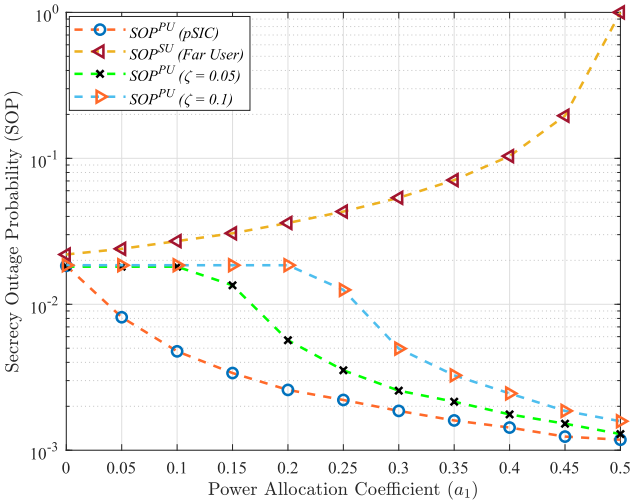

FIGURE 7. PA Coefficient (a_1) Vs secrecy outage probability under both pSIC/ipSIC assumptions.

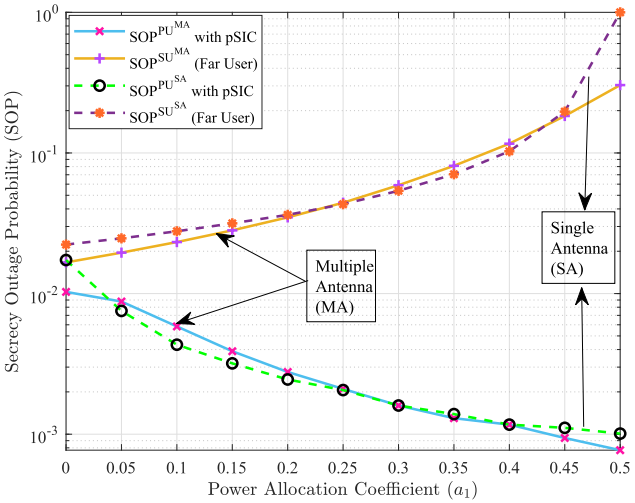

FIGURE 8. PA Coefficient (a_1) Vs secrecy outage probability under multiple antenna case.

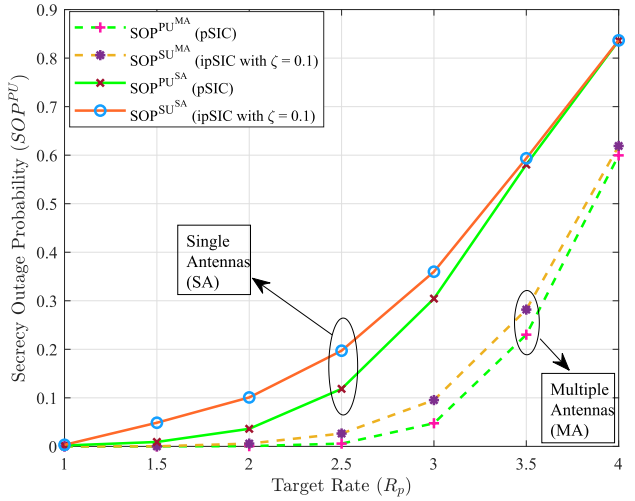

FIGURE 9. Target rate (R_{th}) Vs secrecy outage probability under both pSIC/ipSIC assumptions.

In Fig 7, the SOP of PU/SU is comparable for different values of ζ when PA coefficient i.e., a_1 changes. We set ρ to 20 dBm and look at two situations of SIC imperfections where $\zeta = 0.05$, and $= 0.1$. Based on the data, we can see that the SOP of PU goes down as a_1 increases upto the upper limit of 0.5. This is because the power given to SU goes down as a_1 goes up. So, it becomes more likely that the message x_s won't be decoded and then SOP of PU then goes up. At PA coefficients, it is understood that a certain level of performance can be reached. Also, we can see that as a_1 goes down, the SOP of SU goes down as well. Increasing the strength of the jamming signal to prevent eavesdropping is a simple way to increase security.

In Fig 8, the SOP of PU/SU is comparable for different values of PA coefficient a_1. For a fixed value of transmit SNR (i.e., $\bar{\rho}$ to 20 dBm) and plot the graph for SOP of PU and SU under two SA and MA systems. From the simulation results, we can say that the SOP of PU/SU decreases/increases as a_1 value increases/decreases, respectively as illustrated in Fig 8. Finally, the SOP of PU/SU is intensionally decreases/increases when we vary a_1 value optimally.

The simulated results as illustrated by figures 3 to 8 appear to be better in terms of both accuracy and efficiency when compared to the research works as portrayed in [20] and [21]. Notably, our investigation compares the level of privacy of overlay-CR-NOMA system which is equipped with both SA and MAs over Rayleigh fading channel. When compared with the aforementioned research works, our outcomes achieved better performance. As an illustration, for instance, if we consider Fig. 4, SOP of PU/SU at $\bar{\rho} = 10$dB are 0.8726/0.66726 with SA and 0.0092/0.11665 with MA cases. On the other hand, SOP varies from 0.9-0.7 in [20] and from 0-0.4 in [21].

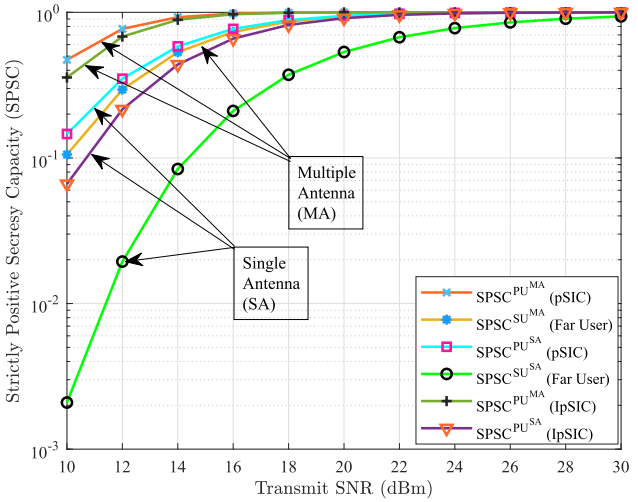

FIGURE 10. Transmit SNR Vs SPSC under both SA and MA Case (s).

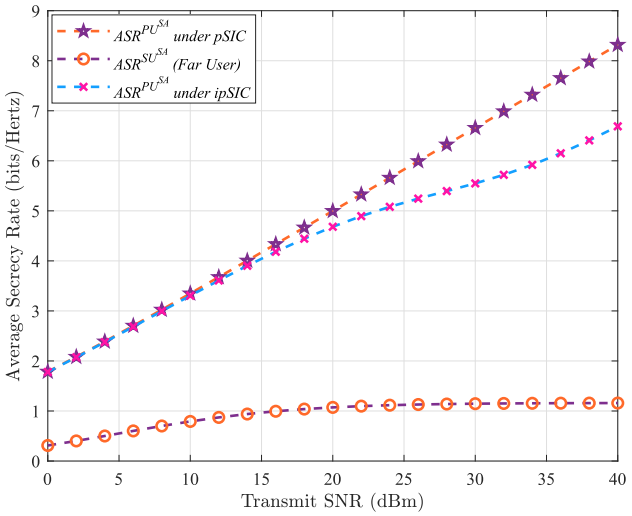

FIGURE 11. Average SNR Vs ASR of both the *NU* & *FU* users under pSIC/ipSIC.

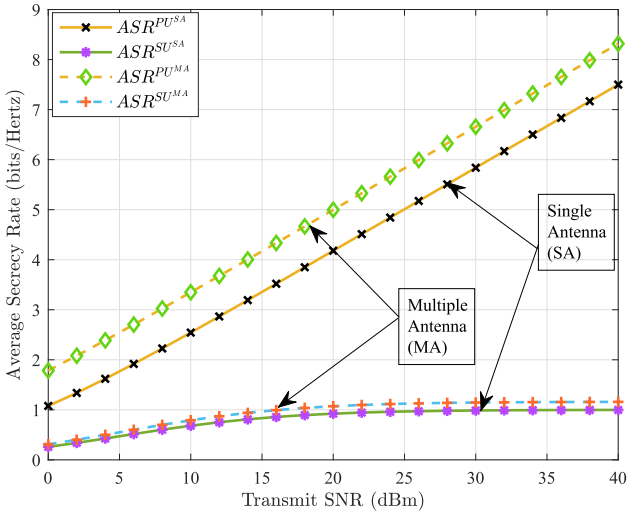

FIGURE 12. Average SNR Vs ASR of both the SU & PU users under multiple antenna case.

In addition, we employed both MRC and SC diversity techniques and derived both exact and asymptotic expressions for the performance metrics. Furthermore, from the simulation results, it can be deduced that our work achieves lower $\bar{\rho}$ values than what is presented in [20] and [21]. In addition, our study derives and validates the expressions corresponding to SPSC and ASR. Nevertheless, those parameters were not considered in the aforementioned works by [20] and [21].

As seen in Fig 9, the only way the SOP changes noticeably is if the target rate is changed under both pSIC ($\zeta = 0$) and ipSIC ($\zeta = 0.1$), respectively. The target rate of PU, i.e., R_p, changes from 1 to 4 and must be determined in order to analyse outage performance under SA, MA cases, are indicated by the values in both (26), (58), respectively. At $R_p = 4$, it is clear that our system is very close to an outage event. This primary result confirms that the proposed overlay CR-NOMA system's outage performance suffers from the higher target rates that are required. This finding prompted us to investigate additional essential variables that, when combined with acceptable controls over related coefficients, can ensure reliable performance. As can be seen in the subsequent simulation results, the outage probability is critical to the computation of the ergodic and effective rates.

The Fig 10, illustrates that the SPSC performance of PU and SU is plotted as a function of transmit SNR under pSIC/ipSIC scenarios. The assessment comparison of our suggested overlay CR-NOMA system equipped with SA and MA is simulated under the presence of the Eve node. The results obtained in Fig 6 clearly shows that under the influence of MA system our proposed system exhibits improved SPSC performance both of PU and SU than the system equipped with SA, this means that at low SNR levels SPSC is enhanced due to improved diversity gain. Therefore, in the suggested approach with MA system, an artificial jamming signal is utilised to guarantee safe reception. Our investigation is confirmed by the conformance between the mathematical and the simulation outcomes for the suggested system.

In Fig. 11, the average secrecy rates comparison of both PU and SU for the proposed overlay CR-NOMA downlink system under pSIC/ipSIC is shown as a function of transmit SNR over Rayleigh fading channel, wherein the outcomes of the analyses performed deploying equations (54), and (58), have been verified via experiments conducted in MATLAB. As $\bar{\rho}$ raising along with the ASR of each of the users exponentially. The achievable SEC of PU of the proposed system outperforms than that SU under pSIC/ipSIC respectively, and than OMA system over Rayleigh fading channel.

In Fig. 12, our proposed overlay CR-NOMA system is shown where the average secrecy rate performances

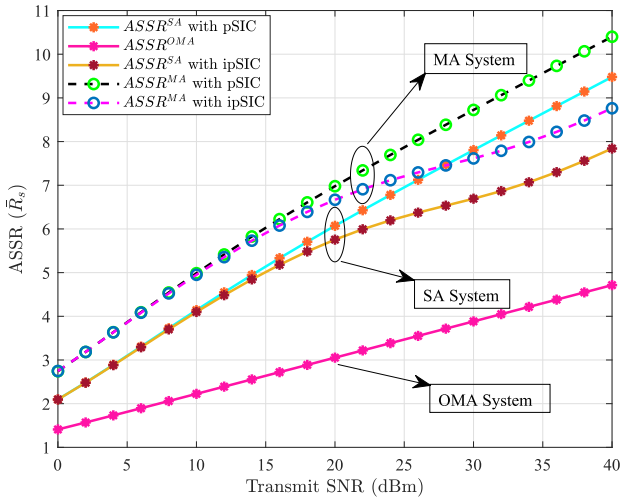

FIGURE 13. Average SNR Vs ASSR under SA as well as MA systems with pSIC/ipSIC assumptions.

comparison between two user is plotted under single and multiple antenna cases over Rayleigh fading channel. The outcomes of the analyses performed deploying equations (63), (67), (106), and (111), respectively, have been verified via experiments conducted in MATLAB. As $\bar{\rho}$ rises the ASR of each user also rises gradually. The graphs that are provided for the ASR of the SA structure have been exhibited simply the sake of contrast, and the achievement of the SA structure is worse compared to that of the MA scenario. The achievable ASR of PU of the proposed system outperforms than that SU under both SA and MA cases, respectively, and than SA system over Rayleigh fading channel.

As Fig. 13 shows that the performance of ASSR under SA/MA cases is plotted as function of $\bar{\rho}$ over Rayleigh fading channel under both pSIC/ipSIC assumptions, wherein the outcomes of the analyses performed deploying equations (68), (1112), respectively, and have been verified via experiments conducted in MATLAB. As $\bar{\rho}$ raising along with the ASR of each of the users exponentially. The achievable ASSR of PU performs better than SU under both pSIC/ipSIC assumptions, respectively, and OMA system over Rayleigh fading channel.

VI. CONCLUSION

In this work, we have proposed a downlink overlay secure CR-NOMA scheme with MA/SA at the primary/secondary transmitters, the secrecy performance comparison between two users PU and SU are obtained under pSIC and ipSIC modes, respectively. This paper investigates the secrecy performance of proposed downlink CR-NOMA system equipped with SA in terms of few performance metrics such as ASR, ASSR, SPSC, SOP, etc. To characterize the secrecy performance of the proposed CR-NOMA network, the novel closed-form analytical expressions of the exact/asymptotic SOP/SPSC and the ASR/ASSR are derived under the both pSIC and ipSIC scenarios.

Furthermore, we extend our proposed work with SA's to MA scenario, where MA's are exploited at the PT as well ST, respectively, for the sake of providing cooperative diversity. In addition, we implement both selection combining (SC)/maximal ratio combining (MRC) techniques for processing the received signals at the PU/Eve, which further improves the system's capacity, and enhances the secrecy performance of the proposed system. To this end, a performance comparison for both the system models i.e., SA-based CR-NOMA system and MA-based CR-NOMA system in terms of SOP, SPSC, and ASR has been carried out through analytical and simulation results. Based on the analytical frameworks, the numerical and simulation results are obtained under different network parameters. In this regard, the outcomes of the simulations are shown to prove the reliability of the mathematical analysis and the accuracy of the suggested technique as well. In our future works, we intend to evaluate the secrecy performance of energy harvesting enabled overlay/underlay downlink/uplink CR-NOMA networks with transmit power optimization over different fading channels.

APPENDIX. A

Proposition 1: Let $\gamma_E^{(1)x_p} = \frac{\rho_E |h_{pe}|^2}{1+\rho_j |h_{sue}|^2}$, as we have know that, $|h_{pe}|^2$, and $|h_{sue}|^2$ follows exponential distribution with parameters $\lambda_{pe} = 1/(\beta d_{pe}^{-\alpha})$, $\lambda_{sue} = 1/(\beta d_{sue}^{-\alpha})$, respectively. The PDF of $\gamma_E^{(1)x_p}$ can be calculated as [21],

$$f_{\gamma_E^{(1)x_p}}(\gamma) = A_1 e^{-\gamma K_1}\left[\frac{K_1}{(A_1+\gamma)} + \frac{1}{(A_1+\gamma)^2}\right] \tag{113}$$

where $A_1 = \frac{\rho_E \lambda_{pe}}{\rho_j \lambda_{sue}}$, $K_1 = \frac{1}{\rho_E \lambda_{pe}}$.

Proof: The CDF of $\gamma_E^{(1)x_p}$ can be expressed as,

$$\begin{aligned} F_{\gamma_E}^{(1)x_s}(\gamma) &= \Pr\left(|h_{pe}|^2 < \frac{\gamma\left(1+\rho_j |h_{sue}|^2\right)}{a_2 \rho_E}\right) \\ &= \int_0^{\infty}\left(1 - F_{|h_{pe}|^2}\left(\frac{\gamma\left(1+\rho_j x\right)}{a_2\rho_E}\right)\right) f_{|h_{sue}|^2}(x)\, dx \\ &= 1 - \frac{A_1 \exp\left\{-\frac{\gamma}{a_2 \lambda_{pe} \rho_E}\right\}}{(A_1+\gamma)} \end{aligned} \tag{114}$$

The PDF of $\gamma_E^{(1)x_p}$ can be determined as (113), after applying the derivative of (114).

Proposition 2: Let $\gamma_E^{(2)x_p} = \frac{a_1 \rho |h_{se}|^2}{1+\rho_j |h_{pe}|^2}$, as we have know that, $|h_{se}|^2$, and $|h_{pe}|^2$ follows exponential distribution with parameters $\lambda_{se} = 1/(\beta d_{se}^{-\alpha})$, $\lambda_{pe} = 1/(\beta d_{pe}^{-\alpha})$, respectively. The PDF of $\gamma_E^{(2)x_p}$ can be derived as [21],

$$f_{\gamma_E^{(2)x_p}}(\gamma) = A_2 e^{-\gamma K_2}\left[\frac{K_2}{(A_2+\gamma)} + \frac{1}{(A_2+\gamma)^2}\right] \tag{115}$$

where $A_2 = \frac{\rho_1 \lambda_{se}}{\rho_j \lambda_{pe}}$, $K_2 = \frac{1}{\rho_1 \lambda_{se}}$.

Proof: The CDF of $\gamma_E^{(2)x_p}$ can be expressed as,

$$F_{\gamma_E}^{(2)x_p}(\gamma) = \Pr\left(|h_{se}|^2 < \frac{\gamma\left(1+\rho_j|h_{pe}|^2\right)}{a_2\rho_E}\right)$$
$$= \int_0^\infty \left(1 - F_{|h_{se}|^2}\left(\frac{\gamma\left(1+\rho_j x\right)}{a_2\rho_E}\right)\right) f_{|h_{pe}|^2}(x)\,dx$$
$$= 1 - \frac{A_2 \exp\left\{-\frac{\gamma}{a_2\lambda_{se}\rho_E}\right\}}{(A_2+\gamma)} \tag{116}$$

The $\gamma_E^{(2)x_p}$ PDF is derived as (115) after obtaining the derivative of (116). The CDF of γ_E^{sc} can be evaluated as,

$$F_{\gamma_E}^{sc}(\gamma) = \Pr\left(\gamma_E^{(1)x_p} < \gamma\right)\Pr\left(\gamma_E^{(2)x_p} < \gamma\right)$$
$$= F_{\gamma_E}^{(1)x_p}(\gamma)\, F_{\gamma_E}^{(2)x_p}(\gamma) \tag{117}$$

The PDF of γ_E^{sc} is calculated by applying the derivative to the above CDF expression as,

$$f_{\gamma_E^{sc}}(\gamma) = f_{\gamma_E^{(1)x_p}}(\gamma)\, F_{\gamma_E^{(2)x_p}}(\gamma) + f_{\gamma_E^{(2)x_p}}(\gamma)\, F_{\gamma_E^{(1)x_p}}(\gamma) \tag{118}$$

Proposition 3: The CDFs/PDFs of γ_E^{mrc} under MRC diversity can be respectively, derived as [4],

$$F_{\gamma_E^{mrc}}(\gamma) = \Pr\left(\gamma_E^{(1)x_p} + \gamma_E^{(2)x_p} < \gamma\right)$$
$$F_{\gamma_E^{mrc}}(\gamma) = \Pr\left(\gamma_E^{(1)x_p} < \gamma\right) + \Pr\left(\gamma_E^{(2)x_p} < \gamma\right)$$
$$F_{\gamma_E^{mrc}}(\gamma) = F_{\gamma_E}^{(1)x_p}(\gamma) + F_{\gamma_E}^{(2)x_p}(\gamma)$$
$$F_{\gamma_E^{mrc}}(\gamma) = 2 - \frac{A_1 \exp\left\{-\frac{\gamma}{a_2\lambda_{pe}\rho_E}\right\}}{(A_1+\gamma)} - \frac{A_2 \exp\left\{-\frac{\gamma}{a_2\lambda_{se}\rho_E}\right\}}{(A_2+\gamma)} \tag{119}$$

When differentiating above equation with respect to γ, using (100), (102) will give you the PDFs of γ_E^{mrc} under MRC diversity as follows:

$$f_{\gamma_E^{mrc}}(\gamma) = A_1 e^{-\gamma K_1}\left[\frac{K_1}{(A_1+\gamma)} + \frac{1}{(A_1+\gamma)^2}\right]$$
$$+ A_2 e^{-\gamma K_2}\left[\frac{K_2}{(A_2+\gamma)} + \frac{1}{(A_2+\gamma)^2}\right] \tag{120}$$

APPENDIX. B

Proposition 4: Let us define $\gamma_E^{(1)x_p} = \frac{\rho_E|h_{pe,M}|^2}{1+\rho_j|h_{sue}|^2} = \frac{X}{Y}$, as we have know that, $|h_{pe,M}|^2$ follows Gamma distribution with $(M, \lambda_{sue,M})$, and $|h_{sue}|^2$ follows exponential distribution with $\lambda_{sue} = 1/(\beta d_{sue}^{-\alpha})$, respectively. The PDF of $\gamma_E^{(1)x_p}$ could be derived as [21],

$$f_{\gamma_E}^{(1)x_p}(\gamma) = \frac{M\lambda_{1E}\rho_E\lambda_{pe}\exp(\lambda_{1E})}{\left(1+\rho_E\lambda_{pe}\lambda_{1E}\gamma\right)^{M+1}} \tag{121}$$

where $\lambda_{1E} = \frac{\lambda_{sue}}{\rho_j}$.

Proof: The CDF of $\gamma_E^{(1)x_p}$ can be expressed as,

$$F_{\gamma_E}^{(1)x_p}(\gamma) = \int_0^\infty \frac{x^{M-1}e^{-\frac{x}{\lambda_{pe}\rho_E}}}{(M-1)!\left(\lambda_{pe}\rho_E\right)^M}dy \int_1^{\gamma x} \lambda_{1E}e^{-\lambda_{1E}(y-1)}dx$$
$$= 1 - \frac{e^{\lambda_{1E}}}{(M-1)!\left(\lambda_{pe}\rho_E\right)^M} I_1 \tag{122}$$

where $I_1 = \int_o^\infty x^{M-1}e^{-Sx}dx$, and $S = \frac{1}{\lambda_{pe}\rho_E} + \lambda_{1E}\gamma$. I_1 can be calculated as,

$$I_1 = S^{1-M}\int_0^\infty (Sx)^{M-1}e^{-Sx}dx$$

Let $t = Sx$,

$$I_1 = S^{-M}\int_1^\infty t^{M-1}e^{-t}dy = (M-1)!$$

Now substituting I_1 into (94), we can get,

$$F_{\gamma_E}^{(1)x_p}(\gamma) = 1 - \frac{\exp(\lambda_{1E})}{\left(1+\lambda_{pe}\rho_E\lambda_{1E}\gamma\right)^M} \tag{123}$$

Using the derivative of (94), we get (92) as the PDF of $\gamma_E^{(1)x_p}$.

Proposition 5: Let $\gamma_E^{(2)x_p} = \frac{a_1\rho|h_{se,N}|^2}{1+\rho_j|h_{pe}|^2} = \frac{U}{V}$, as we have know that, $|h_{se,N}|^2$ follows Gamma distribution with $(N, \lambda_{se,N})$, and $|h_{pe}|^2$ follows exponential distribution with $\lambda_{pe} = 1/(\beta d_{pe}^{-\alpha})$, respectively. The PDF of $\gamma_E^{(2)x_p}$ can be calculated as [21],

$$f_{\gamma_E}^{(2)x_p}(\gamma) = \frac{N\rho_1\lambda_{se}\lambda_{2E}\exp(\lambda_{2E})}{(1+\rho_1\lambda_{se}\lambda_{2E}\gamma)^{N+1}} \tag{124}$$

where $\lambda_{2E} = \frac{\lambda_{pe}}{a_1\rho}$.

Proof: The CDF of $\gamma_E^{(2)x_p}$ could be derived as,

$$F_{\gamma_E}^{(2)x_p}(\gamma) = \int_0^\infty \frac{x^{N-1}e^{-\frac{x}{\lambda_{se}\rho_1}}}{(N-1)!(\lambda_{se}\rho_1)^N}dy \int_1^{\gamma x} \lambda_{2E}e^{-\lambda_{2E}(y-1)}dy$$
$$= 1 - \frac{e^{\lambda_{2E}}}{(N-1)!(\lambda_{se}\rho_1)^N} I_2 \tag{125}$$

where $I_2 = \int_o^\infty x^{N-1}e^{-Sx}dx$, and $S = \frac{1}{\lambda_{se}\rho_1} + \lambda_{2E}\gamma$.

I_2 can be calculated as,

$$I_2 = S^{1-N}\int_0^\infty (Sx)^{N-1}e^{-Sx}dx$$

Let $t = Sx$,

$$I_2 = S^{-N}\int_1^\infty t^{N-1}e^{-t}dy = (N-1)!$$

Now substituting I_2 into (96), we can get,

$$F_{\gamma_E}^{(2)x_p}(\gamma) = 1 - \frac{\exp(\lambda_{2E})}{(1+\lambda_{se}\rho_1\lambda_{2E}\gamma)^N} \tag{126}$$

Using the derivative of (97), we get (95) as the PDF of $\gamma_E^{(2)x_p}$. The CDF of γ_E^{sc} could be evaluated as,

$$\begin{aligned} F_{\gamma_E}^{sc}(\gamma) &= \Pr\left(\gamma_E^{(1)x_p} < \gamma\right) \Pr\left(\gamma_E^{(2)x_p} < \gamma\right) \\ &= F_{\gamma_E}^{(1)x_p}(\gamma)\, F_{\gamma_E}^{(2)x_p}(\gamma) \end{aligned} \tag{127}$$

The PDF of γ_E^{sc} is calculated using the expression in (127) as,

$$f_{\gamma_E^{sc}}(\gamma) = f_{\gamma_E^{(1)x_p}}(\gamma)\, F_{\gamma_E^{(2)x_p}}(\gamma) + f_{\gamma_E^{(2)x_p}}(\gamma)\, F_{\gamma_E^{(1)x_p}}(\gamma) \tag{128}$$

REFERENCES

[1] L. Lv, J. Chen, Q. Ni, Z. Ding, and H. Jiang, "Cognitive non-orthogonal multiple access with cooperative relaying: A new wireless frontier for 5G spectrum sharing," *IEEE Commun. Mag.*, vol. 56, no. 4, pp. 188–195, Apr. 2018, doi: 10.1109/MCOM.2018.1700687.

[2] Z. Ding, X. Lei, G. K. Karagiannidis, R. Schober, J. Yuan, and V. K. Bhargava, "A survey on non-orthogonal multiple access for 5G networks: Research challenges and future trends," *IEEE J. Sel. Areas Commun.*, vol. 35, no. 10, pp. 2181–2195, Oct. 2017, doi: 10.1109/JSAC.2017.2725519.

[3] F. Li, H. Jiang, R. Fan, and P. Tan, "Cognitive non-orthogonal multiple access with energy harvesting: An optimal resource allocation approach," *IEEE Trans. Veh. Technol.*, vol. 68, no. 7, pp. 7080–7095, Jul. 2019.

[4] L. Luo, Q. Li, and J. Cheng, "Performance analysis of overlay cognitive NOMA systems with imperfect successive interference cancellation," *IEEE Trans. Commun.*, vol. 68, no. 8, pp. 4709–4722, Aug. 2020, doi: 10.1109/TCOMM.2020.2992471.

[5] A. K. Shukla, V. Singh, P. K. Upadhyay, A. Kumar, and J. M. Moualeu, "Performance analysis of energy harvesting-assisted overlay cognitive NOMA systems with incremental relaying," *IEEE Open J. Commun. Soc.*, vol. 2, pp. 1558–1576, 2021.

[6] Y. Cao, N. Zhao, Y. Chen, M. Jin, Z. Ding, Y. Li, and F. R. Yu, "Secure transmission via beamforming optimization for NOMA networks," *IEEE Wireless Commun.*, vol. 27, no. 1, pp. 193–199, Feb. 2020.

[7] N. Zhao, D. Li, M. Liu, Y. Cao, Y. Chen, Z. Ding, and X. Wang, "Secure transmission via joint precoding optimization for downlink MISO NOMA," *IEEE Trans. Veh. Technol.*, vol. 68, no. 8, pp. 7603–7615, Aug. 2019.

[8] S. Thakur, A. Singh, and S. Majhi, "Secrecy analysis of underlay CRN in the presence of correlated and imperfect channel," *IEEE Trans. Cogn. Commun. Netw.*, vol. 9, no. 3, pp. 754–764, Jun. 2023.

[9] K. Cao, B. Wang, H. Ding, L. Lv, J. Tian, and F. Gong, "On the security enhancement of uplink NOMA systems with jammer selection," *IEEE Trans. Commun.*, vol. 68, no. 9, pp. 5747–5763, Sep. 2020.

[10] S. Sharma, S. D. Roy, and S. Kundu, "Secrecy at physical layer in NOMA with cooperative jamming," in *Proc. Nat. Conf. Commun. (NCC)*, Feb. 2020, pp. 1–6.

[11] Y. Liu, Z. Ding, M. Elkashlan, and J. Yuan, "Nonorthogonal multiple access in large-scale underlay cognitive radio networks," *IEEE Trans. Veh. Technol.*, vol. 65, no. 12, pp. 10152–10157, Dec. 2016.

[12] S. Arzykulov, T. A. Tsiftsis, G. Nauryzbayev, M. Abdallah, and G. Yang, "Outage performance of underlay CR-NOMA networks with detect-and-forward relaying," in *Proc. IEEE Global Commun. Conf. (GLOBECOM)*, Dec. 2018, pp. 1–6.

[13] A. Aswathi and A. V. Babu, "Performance analysis of NOMA-based underlay cognitive radio networks with partial relay selection," *IEEE Trans. Veh. Technol.*, vol. 70, no. 5, pp. 4615–4630, May 2021.

[14] Z. Xiang, W. Yang, G. Pan, Y. Cai, and Y. Song, "Physical layer security in cognitive radio inspired NOMA network," *IEEE J. Sel. Top. Signal Process.*, vol. 13, no. 3, pp. 700–714, Jun. 2019.

[15] D.-T. Do, M.-S. V. Nguyen, F. Jameel, R. Jantti, and I. S. Ansari, "Performance evaluation of relay-aided CR-NOMA for beyond 5G communications," *IEEE Access*, vol. 8, pp. 134838–134855, 2020.

[16] H. Huang, Y. Shi, L. Liang, J. He, and X. Zhang, "Performance analysis of overlay cognitive NOMA network with imperfect SIC and imperfect CSI," *Phys. Commun.*, vol. 53, Aug. 2022, Art. no. 101711.

[17] S. Arzykulov, T. A. Tsiftsis, G. Nauryzbayev, and M. Abdallah, "Outage performance of cooperative underlay CR-NOMA with imperfect CSI," *IEEE Commun. Lett.*, vol. 23, no. 1, pp. 176–179, Jan. 2019.

[18] G. Im and J. H. Lee, "Outage probability for cooperative NOMA systems with imperfect SIC in cognitive radio networks," *IEEE Commun. Lett.*, vol. 23, no. 4, pp. 692–695, Apr. 2019.

[19] B. M. ElHalawany, A. A. A. El-Banna, Q.-V. Pham, K. Wu, and E. M. Mohamed, "Spectrum sharing in cognitive-radio-inspired NOMA systems under imperfect SIC and cochannel interference," *IEEE Syst. J.*, vol. 16, no. 1, pp. 1540–1547, Mar. 2022, doi: 10.1109/JSYST.2021.3131122.

[20] D. Jiang, Y. Gao, N. Sha, X. Wang, and N. Li, "Physical layer security of cooperative NOMA systems with an untrusted user," in *Proc. IEEE 22nd Int. Conf. Commun. Technol. (ICCT)*, Nanjing, China, Nov. 2022, pp. 1287–1292, doi: 10.1109/ICCT56141.2022.10073079.

[21] B. C. Chen, R. Li, Q. Ning, K.-J. Lin, C. Han, and V. C. M. Leung, "Security at physical layer in NOMA relaying networks with cooperative jamming," *IEEE Trans. Veh. Technol.*, vol. 71, no. 4, pp. 3883–3888, Apr. 2022.

[22] L. Alberto, *Probability, Statistics, and Random Processes for Electrical Engineering*, 3rd ed. Upper Saddle River, NJ, USA: Prentice-Hall, 2008.

[23] M. Abramowitz and I. Stegun, *Handbook of Mathematical Functions With Formulas, Graphs, and Mathematical Tables*, 1st ed. New York, NY, USA: Dover, 1972.

[24] X. Liu, "Probability of strictly positive secrecy capacity of the Rician–Rician fading channel," *IEEE Wireless Commun. Lett.*, vol. 2, no. 1, pp. 50–53, Feb. 2013.

[25] M. V. Nguyen, D.-T. Do, F. Afghah, S. M. R. Islam, and A.-T. Le, "Exploiting secrecy performance of uplink NOMA in cellular networks," *IEEE Access*, vol. 9, pp. 95135–95154, 2021.

[26] X. Xie, J. Liu, J. Huang, and S. Zhao, "Ergodic capacity and outage performance analysis of uplink full-duplex cooperative NOMA system," *IEEE Access*, vol. 8, pp. 164786–164794, 2020.

[27] I. S. Gradshteyn and I. M. Ryzhik, *Table of Integrals, Series and Products*, 7th ed. San Diego, CA, USA: Elsevier, Mar. 2007.

[28] D. H. Tashman, "Physical-layer security in cognitive radio networks," Ph.D thesis, Dept. Elect. Comput. Eng., Concordia Univ., Montreal, QC, Canada, Apr. 2022.

[29] Md. F. Kader and S. Y. Shin, "Coordinated direct and relay transmission using uplink NOMA," *IEEE Wireless Commun. Lett.*, vol. 7, no. 3, pp. 400–403, Jun. 2018.

[30] T. Thapar, D. Mishra, D. W. K. Ng, and R. Saini, "Secrecy outage probability analysis for downlink untrusted NOMA under practical SIC error," in *Proc. IEEE GLOBECOM*, Madrid, Spain, Dec. 2021, pp. 1–6 doi: 10.1109/GLOBECOM46510.2021.9685578.

[31] H. Lei, F. Yang, I. S. Ansari, H. Liu, K. J. Kim, and T. A. Tsiftsis, "Secrecy outage performance analysis for uplink CR-NOMA systems with hybrid SIC," *IEEE Internet Things J.*, vol. 10, no. 15, pp. 13181–13195, Aug. 2023, doi: 10.1109/JIOT.2023.3261308.

[32] S. Thakur and A. Singh, "Secrecy performance of underlay cognitive radio networks with primary interference," *IEEE Trans. Netw. Sci. Eng.*, vol. 9, no. 4, pp. 2641–2657, Jul. 2022, doi: 10.1109/TNSE.2022.3168268.

[33] A. Souzani, M. A. Pourmina, P. Azmi, and M. Naser-Moghadasi, "Physical layer security enhancement via IRS based on PD-NOMA and cooperative jamming," *IEEE Access*, vol. 11, pp. 65956–65967, 2023, doi: 10.1109/ACCESS.2023.3290104.

[34] Y. Pei, X. Yue, W. Yi, Y. Liu, X. Li, and Z. Ding, "Secrecy outage probability analysis for downlink RIS-NOMA networks with on-off control," *IEEE Trans. Veh. Technol.*, vol. 72, no. 9, pp. 11772–11786, Sep. 2023, doi: 10.1109/TVT.2023.3267531.

[35] C. Gong, X. Yue, Z. Zhang, X. Wang, and X. Dai, "Enhancing physical layer security with artificial noise in large-scale NOMA networks," *IEEE Trans. Veh. Technol.*, vol. 70, no. 3, pp. 2349–2361, Mar. 2021, doi: 10.1109/TVT.2021.3057661.

[36] S. Gadi, S. P. Singh, A. Kumar, R. K. Singh, and G. Singh, *IET Commun.*, vol. 17, no. 19, pp. 2188–2199, Dec. 2023, doi: 10.1049/cmu2.12689.

[37] E. Li, Z. Liang, Y. Wang, and M. Zheng, "Enhancing the secrecy performance of two-way relay systems with eavesdropping user," *Phys. Commun.*, vol. 61, Dec. 2023, Art. no. 102216.

[38] Z. Xie, Y. Liu, W. Yi, X. Wu, and A. Nallanathan, "Physical layer security for STAR-RIS-NOMA: A stochastic geometry approach," 2023, *arXiv:2304.06128*.
[39] Z. Chen, N. Zhao, D. K. C. So, J. Tang, X. Y. Zhang, and K.-K. Wong, "Joint altitude and hybrid beamspace precoding optimization for UAV-enabled multiuser mmWave MIMO system," *IEEE Trans. Veh. Technol.*, vol. 71, no. 2, pp. 1713–1725, Feb. 2022, doi: 10.1109/TVT.2021.3134044.
[40] L. Zhu, J. Zhang, Z. Xiao, X. Cao, D. O. Wu, and X.-G. Xia, "3-D beamforming for flexible coverage in millimeter-wave UAV communications," *IEEE Wireless Commun. Lett.*, vol. 8, no. 3, pp. 837–840, Jun. 2019, doi: 10.1109/LWC.2019.2895597.
[41] R. Negi and S. Goel, "Secret communications using artificial noise," in *Proc. IEEE VTC*, Dallas, TX, USA, Sep. 2005, pp. 1906–1910.
[42] S. Goel and R. Negi, "Guaranteeing secrecy using artificial noise," *IEEE Trans. Wireless Commun.*, vol. 7, no. 6, pp. 2180–2189, Jun. 2008.
[43] A. L. Swindlehurst, "Fixed SINR solutions for the MIMO wiretap channel," in *Proc. IEEE Int. Conf. Acoust., Speech Signal Process.*, Taipei, Taiwan, Apr. 2009, pp. 2437–2440.

KIRAN KUMAR GODUGU (Graduate Student Member, IEEE) received the B.Tech. degree in electronics and communication engineering from Jawaharlal Nehru Technological University Hyderabad, India, in 2008, and the M.Tech. degree from SRM University, Chennai, Tamil Nadu, India, in 2011. He is currently pursuing the Ph.D. degree (internal full-time) with the School of Electronics Engineering, VIT-AP University, Amaravati, Andhra Pradesh, India. He was an Assistant Professor, from 2011 to 2021, in various engineering colleges in Hyderabad, India. His research interests include spectrum sensing issues and fading models in cognitive radio networks (CRNs) and investigations on resource allocation of non-orthogonal multiple access techniques (NOMA), cooperative NOMA, physical layer security (PLS), simultaneous wireless information and power transfer (SWIPT), and overlay/underlay cognitive radio (CR) inspired NOMA (CR-NOMA) systems. As of today, he has published three SCI journals, and a seven IEEE conference papers.

SUSEELA VAPPANGI (Member, IEEE) received the B.Tech. degree in electronics and communication engineering and the M.Tech. degree in the stream of communications and signal processing from Jawaharlal Nehru Technological University Hyderabad, India, in 2013 and 2015, respectively, and the Ph.D. degree from the National Institute of Technology Warangal, India. Currently, she is with VIT-AP University as an Assistant Professor. Her research interests include signal processing for communications, communications with major emphasis on modulation and broadband wireless communications, and visible light communications.